Available online at www.sciencedirect.com
ScienceDirect
Developmental Biology 316 (2008) 171–190
DEVELOPMENTAL BIOLOGY
www.elsevier.com/developmentalbiology

A nutritional model of late embryonic vitamin A deficiency produces defects in organogenesis at a high penetrance and reveals new roles for the vitamin in skeletal development

Angela Wai-Man See [a], Mary E. Kaiser [b], Jeffrey C. White [c], Margaret Clagett-Dame [a,b,c,*]

[a] *Interdepartmental Graduate Program in Nutritional Sciences, University of Wisconsin-Madison, Madison, WI 53706-1544, USA*
[b] *Department of Biochemistry, University of Wisconsin-Madison, Madison, WI 53706-1544, USA*
[c] *Pharmaceutical Science Division, University of Wisconsin-Madison, Madison, WI 53706-1544, USA*

Received for publication 25 May 2007; revised 18 September 2007; accepted 16 October 2007
Available online 23 October 2007

Abstract

Vitamin A plays an essential role in vertebrate embryogenesis. In the present study, pregnant vitamin A-deficient (VAD) rats were maintained during early pregnancy on the short half-life vitamin A metabolite, all-*trans* retinoic acid (atRA), in an amount sufficient to support normal development to E10.5, with a higher level of atRA (250 μg atRA/g diet) provided from embryonic day (E) 8.5–10.5 to prevent mid-gestational resorption. When limiting amounts of atRA (1.5 or 12 μg/g diet) were provided after E10.5, a highly reproducible and penetrant state of late fetal vitamin A deficiency (late VAD) was induced in the organs of developing fetuses. In addition, late VAD fetuses displayed both anteriorization of cervical regions and novel posteriorization events at the thoracic and sacral levels of the skeleton, and showed sternal and pelvic malformations not previously observed in early VAD or genetic models. The expression of several *Hox* genes (*Hoxd3* and *Hoxb4*) was altered in late VAD embryos, with a reduction in *Hoxd3* noted as early as 1 day after instituting deficiency. All late VAD-induced malformations were prevented by the addition of retinol starting at E10.5, whereas provision of a high level of atRA throughout pregnancy improved but could not completely rescue the development of all organ systems. This work defines a nutritional model in which vitamin A deficiency can be induced during fetal development, and reveals new functions for the vitamin in the development of the axial and appendicular skeleton.

Keywords: Anteriorization; Embryonic development; Homeotic transformation; *Hox* gene; Organogenesis; Posteriorization; Retinoic acid; Rib fusion; Skeletal development; Sternum; Vitamin A deficiency

Introduction

Vitamin A (retinol) is essential for vertebrate embryogenesis (McCaffery and Drager, 2000; Zile, 2001; Clagett-Dame and DeLuca, 2002; Mark et al., 2006) and severe vitamin A deficiency leads to complete reproductive failure in the female (Evans, 1928). Vitamin A is normally obtained in the diet in the form of retinyl ester or carotenoid and both are metabolized to retinol. Retinol is stored as an ester in tissues, and is metabolized when needed to retinaldehyde and further oxidized to all-*trans* retinoic acid (atRA). atRA is believed to support all known functions of vitamin A in mammals with the exception of vision, although other retinol metabolites have been reported to have biological activity *in vitro* (Moise et al., 2007). A large body of work supports numerous roles for atRA in early developmental processes, whereas less is known about the functions of vitamin A at later times in fetal development.

Studies in the 1940s and 50s provided the first evidence that vitamin A is needed to support fetal development in the rat (Warkany and Schraffenberger, 1944, 1946; Wilson and Warkany, 1948, 1949; Wilson et al., 1953). In these studies, a large number of female weanling rats were fed a vitamin A-deficient (VAD) diet and supplemented with small amounts of β-carotene (and in some cases ground horse muscle) before mating. Of the pregnant animals, over half either died or re-

* Corresponding author. Department of Biochemistry, University of Wisconsin-Madison, 433 Babcock Drive, Madison, WI 53706-1544, USA. Fax: +1 608 262 7122.
E-mail address: dame@biochem.wisc.edu (M. Clagett-Dame).

0012-1606/$ - see front matter © 2007 Elsevier Inc. All rights reserved.
doi:10.1016/j.ydbio.2007.10.018

sorbed their embryos completely before embryonic day 14 (E14). Fetuses were removed from mothers showing abnormal bleeding (indicative of the onset of resorption) and upon more detailed histological examination, a variety of organ defects were reported and coined the "vitamin A deficiency syndrome". However, the penetrance of the defects across the embryos surveyed was highly variable ranging from 4% to 42% for most systems (urogenital organs, kidneys, diaphragm and lung; Wilson et al., 1953). Thus, in these early studies, the severity of the deficiency varied from animal to animal, in large part because β-carotene can be converted to retinol and stored. This nutritional approach to study the effect of VAD on organogenesis was therefore limited by its lack of penetrance and the variable nature of the timing of deficiency.

In 1946, Arens and van Dorp reported the synthesis of atRA, and subsequent studies showed that it could support the growth of VAD animals (Arens and van Dorp, 1946a,b). Later studies revealed that the amount of atRA that would support growth in the non-pregnant animal (2–12 μg/g diet or ~40–230 μg/rat/day) could also support the early but not later stages of pregnancy. When this amount of atRA was provided to the pregnant VAD mother, embryos formed, but the conceptus was always resorbed at midgestation (Thompson et al., 1964; White et al., 1998). More recently, our group has shown that supplementation of VAD rats with an even higher level of atRA (250 μg/g diet or ~4 mg/rat/day), either from the onset of pregnancy or after E8.5, can prevent embryonic resorption at midgestation (White et al., 1998, 2000). The need for higher amounts of atRA starting at the late gastrula (presomite stage) to neurula stage coincides with the time when the rodent embryo begins to synthesize its own atRA (Rossant et al., 1991; Niederreither et al., 1997; Ulven et al., 2000). White et al. (2000) showed that if female VAD rats are fed atRA at a level of 12 μg/g diet from E0.5 to 8.5 and 250 μg atRA/g diet from E8.5 to 10.5 followed by daily oral dosing with retinyl palmitate (RP), live offspring are produced that give rise to a second generation. Thus, simply by increasing the maternal intake of atRA at this critical time, fetal resorption at later times can be overcome and development can proceed.

In the present study, we describe a nutritional model that produces late VAD in rat fetuses with defects in organogenesis that are highly reproducible and fully penetrant. In this model, pregnant VAD animals are supported during early gestation (E0.5 to E8.5) on an adequate level of atRA followed by the feeding of higher atRA through approximately the 12- to 15-somite stage to prevent mid-gestational death. Placing the animals on a lower level of dietary atRA after E10.5 produces a state of late fetal VAD, whereas supplementation with retinol (RP) after E10.5 yields fetuses that appear histologically normal at E18.5 and E21.5. The model takes advantage of the short biological half-life of atRA and the fact that this metabolite is not stored, thus enabling production of VAD at a precise time in later development. Using this late VAD rat model, unique defects in the thoracic, sacral and pelvic regions of the developing skeleton are also revealed.

Materials and methods

Generation of rat embryos

Female rats (Harlan Sprague-Dawley, Madison, WI) were depleted of vitamin A as previously described (White et al., 1998). The VAD rats were placed back on a maintenance level of atRA (12 μg atRA/g diet) for a minimum of 2 weeks prior to mating; E0.5 was defined as 12 p.m. of the day that the rat was determined to be sperm-positive. The rats were then assigned to the dietary treatment groups shown in Fig. 1. Analysis of the atRA content of the diet was carried out as described previously and was found to be ±10% of the desired value (White et al., 1998). Food intake was measured daily from E0.5 to the day of sacrifice. In the high atRA-containing diet group (250 μg/g), only animals that consumed at least 11 g of food/day from E8.5 to E10.5 were

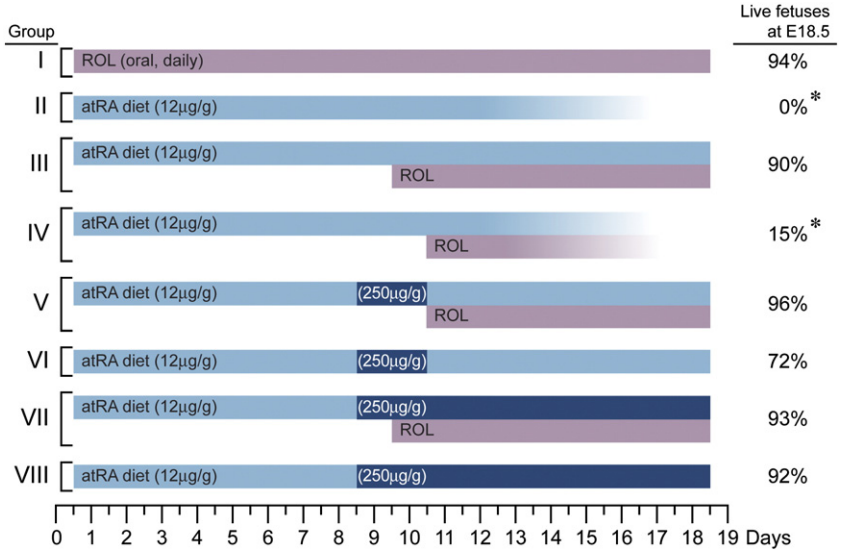

Fig. 1. Maternal dietary treatment groups and fetal outcome at embryonic day (E) 18.5. VAD rats were fed diets containing one of two atRA levels and/or were dosed orally with 500 IU of retinol (ROL) per day in the form of retinyl palmitate and were sacrificed at E18.5. Fetal survival is shown in the right-hand column {% Live fetuses = [live/(live+dead+resorbed)]×100%}. The mean number of live fetuses/litter in groups I–VIII was 11, 0, 10, 1, 8, 9, 9 and 11, respectively. The number of litters analyzed for each group (I–VIII) was 3, 3, 4, 4, 3, 3, 4, and 4, respectively. atRA, all-*trans* retinoic acid; IU, international units. *p value <0.05 compared with group I.

included in the analysis to insure adequate retinoid intake; food intake averaged 16±2 g/day.

Histological analysis of the embryos

At either E18.5 or E21.5, pregnant rats were sacrificed and the anaesthetized fetuses were fixed in Bouin's solution (VWR Scientific Products, West Chester, PA) or ethanol at 4 °C. Bouin's-fixed fetuses were washed in phosphate-buffered saline at 4 °C, dehydrated to 100% ethanol, embedded in paraffin under vacuum and sectioned transversely at 10 μm. Sections were stained using Groat's Hematoxylin and Mallory's Trichrome stain (Mark et al., 1993). For skeletal analysis, E21.5 fetuses were partially skinned, fixed in ethanol and stained for bone and cartilage using Alcian blue and Alizarin red as described previously (Lufkin et al., 1992). Five to seven fetuses from three separate litters were sectioned for each treatment group and time point, and 6 to 12 fetuses from 3 to 6 litters were stained for bone and cartilage in each treatment group. Comparative images of various skeletal regions were taken at the same magnification. Measurement of the dentary, nasal and incisor bones was made from digital images using MetaMorph software (Universal Imaging Corporation, West Chester, PA). Fetal survival and bone length were analyzed using a one-way analysis of variance (ANOVA) followed by pairwise comparisons (Tukey's HSD, Sheffe's Test and Fisher's test; significance set at $P<0.05$).

In situ hybridization analysis of embryos

In situ hybridization of whole rat embryos (E11.5–E13.5) and floating sections (E15.5 and E16.5) was performed as described (Kaiser et al., 2003). The *Hoxd3* and *Hoxd4* ribroprobes were generated as described (Kaiser et al., 2003) and a 337-bp rat *Wnt3a* probe was prepared using a cDNA generated by PCR using the primers: 5′-*attcccagagcctgctgttca*-3′ and 5′-*atcacttttgtctaaatccagtg*-3′. The *Hoxb4* probe was a kind gift from Dr. R. Krumlauf (Stowers Institute, Kansas City, MO). For vibratome sections, embryos were embedded in 3% agarose in PBS at 65 °C and stored overnight at 4 °C prior to sectioning.

Results

The addition of either ROL or a high level of atRA at the late gastrula/early neural stage supports fetal survival to E18.5

The result of supplementing the diets of VAD rats with either atRA (12 or 250 μg/g) and/or giving oral retinol (ROL) at various times during pregnancy on fetal outcome (percent live fetuses) at E18.5 is shown in the right column in Fig. 1. The administration of ROL to VAD rats starting at the onset of pregnancy or E0.5 (group I) yielded live fetuses (94%) when assessed at E18.5. In contrast, no live fetuses were present in the group maintained on the low level of atRA (12 μg/g diet; group II). This level of atRA has been shown previously to be insufficient to support embryo survival beyond midgestation, and thus served as a control to verify that the rats were depleted of vitamin A stores prior to mating (White et al., 1998). When ROL was added at E9.5 (group III), the majority of fetuses taken at E18.5 were alive (90%), whereas if the addition of ROL was delayed by 1 day (E10.5), nearly all fetuses were resorbed (group IV). In order to determine whether atRA could substitute for ROL during this critical time, a pharmacological amount of atRA (250 μg atRA/g diet) was given from E8.5 to E10.5 and was followed by daily supplementation with ROL starting at E10.5 (group V). Because the diet served as the means to deliver atRA, it was made available to the pregnant animals starting at E8.5 to insure that sufficient retinoid was available during the critical E9.5–E10.5 window of time. This resulted in normal fetal survival (96%) showing that the addition of the pharmacological amount of atRA was able to substitute for ROL, at least until E10.5, and thus, late fetal resorption that normally occurs when retinoid is limiting was prevented. In the key group VI, we sought to institute a state of late VAD by feeding the pharmacological amount of atRA (250 μg atRA/g diet) from E8.5 to E10.5 (to prevent early VAD-induced fetal resorption), followed by feeding of the low level of atRA (12 μg/g diet) until E18.5. Provision of the pharmacological amount of atRA during this short, but critical window of time (E8.5–10.5) enabled the majority of fetuses (72%) to survive to E18.5. This work showed that it was possible to prevent late fetal resorption that normally accompanies early vitamin A-deficiency during pregnancy by adding a high level of supplemental atRA starting at the late gastrula/early neurula stage in the developing rat embryo. The ability to overcome VAD-induced fetal resorption enabled us to produce a well-defined and reproducible state of vitamin A deficiency during later stages of embryonic development; the detailed morphology of these fetuses will be discussed below.

Two additional groups were given the pharmacological amount of atRA (250 μg/g diet) for a more extended period, from E8.5 to E18.5, either with (group VII) or without (group VIII) supplemental ROL starting at E9.5. Both dietary regimens supported fetal survival to E18.5 (93% and 92%, respectively, similar to that of groups I, III, V and VI). These fetuses were also examined in detail to determine if a high level of atRA alone could support organ development to E18.5, and if not, whether the outcome was improved if ROL was also provided concurrently.

Severe abnormalities result from late vitamin A deficiency

The development of a variety of organs and tissues from fetuses in groups I to VIII were scored as morphologically normal (Tables 1 and 2; open box), severely abnormal (black box) or having a developmental defect that was still apparent, but showing some rescue in development (grey box) compared to that defined as severely abnormal. These results show that normal embryonic development is supported in full to E10.5 by atRA (low level E0.5 to E8.5 and high from E8.5 to E10.5), after which time limiting the amount of atRA induces a highly penetrant state of late fetal deficiency (group VI; Tables 1 and 2).

Eye, nasal and salivary gland development

All fetuses (6/6) in the late VAD group (VI) developed severe eye and nasal abnormalities by E18.5 (Figs. 2C, F and Table 1) whereas development of these tissues was normal in the VAS groups that received ROL starting either at the onset of pregnancy (group I; Figs. 2A, D and Table 1) or after E9.5 (group III; data not shown). The vitamin A sufficient (VAS) fetuses had closed eyelids, a well-formed retina containing two layers, and two cell-free regions – the anterior chamber and the vitreous body (Fig. 2A). Eye morphology in the group V fetuses was similar in all respects to that of the VAS groups I and III. In contrast, 100% of the late VAD fetuses (group VI; Fig. 2C) had

Table 1
Summary of the defects in the head and neck region of late VAD fetuses

	Group						VAD syndrome	Genetic models
	I	III	V	VI	VII	VIII		
Eye								
Eversion and/or folding of the neural retina	6	7	5	6	6	3 2 1	Yes[a,b]	Yes[c]
	0%	0%	0%	100%	0%	50%	94%	
Thickening of neural retina	6	7	5	6	6	2 4	NR	Yes[d]
	0%	0%	0%	0%	0%	67%		
Fibrous retrolenticular membrane	6	7	5	6	6	2 3 1	Yes[a,b]	Yes[c,e]
	0%	0%	0%	100%	0%	67%	100%	
Unfused eyelids	6	7	5	6	6	4 2	Yes[a,b]	Yes[c]
	0%	0%	0%	100%	0%	33%	53%	
Small conjunctival sac	6	7	5	6	6	5 1	Yes[b]	Yes[c]
	0%	0%	0%	100%	0%	17%	56%	
Corneal-lenticular stalk	6	7	5	6	6	2 2 2	Yes[a,b]	Yes[c]
	0%	0%	0%	100%	0%	67%		
Absence of the anterior chamber	6	7	5	6	6	2 1 3	Yes[a,b]	Yes[c]
	0%	0%	0%	100%	0%	67%	88%	
Absence of the vitreous body	6	6 1	5	6	6	4 1 1	Yes[a,b]	Yes[c]
	0%	14%	0%	100%	0%	33%	88%	
Rudimentary or loss of iris	6	7	5	6	6	2 4	Yes[b]	Yes[c]
	0%	0%	0%	100%	0%	67%	88%	
Head and Neck								
Nasal region less developed	6	7	5	2 4	7	1 5	NR	Yes[e]
	0%	0%	0%	100%	0%	83%		
Salivary glands hypoplastic or missing	6	7	5	6	7	4 2	NR	Yes[c]
	0%	0%	0%	100%	0%	100%		

Organs and tissues were scored as normal (open box), mildly abnormal (grey box), or severely abnormal (black box). The percentage of fetuses showing any abnormality (mild or severe) is shown underneath the box.
[a]Warkany and Schraffenberger (1944); [b]Warkany and Schraffenberger (1946); [c]Lohnes et al. (1994); [d]Molotkov et al. (2006); [e]Dupe et al. (2003).

open eyelids, severe folding and eversion of the neural retina, the anterior chamber of the eye was missing and the lens was fused with the cornea (Fig. 2C). In the late VAD fetuses, both the size of the nasal turbinate cartilage and nasal cavity were severely reduced, and the serous glands (Fig. 2F) and salivary glands (data not shown) were missing in all fetuses. Importantly, the addition of ROL after E10.5 (group V) rescued all of the eye (Fig. 2B and Table 1), nasal, and glandular defects (Fig. 2E and data not shown) observed in the late VAD group, confirming that the defects observed in group VI were attributable to retinoid deficiency imposed after this time.

Lung, diaphragm, and cardiac development

All of the fetuses in the late VAD group VI showed severe abnormalities in the lung and diaphragm, and to a much lesser extent, in cardiac development (Table 2). In the VAS groups (I, III and V) the left lung was composed of one lobe and the right lung had four lobes (cranial, caudal, middle, and accessory; Figs. 2G, H, and data not shown). All of the late VAD group VI fetuses showed bilateral hypoplasia of the left, cranial and caudal lobes, with nearly a complete loss of the accessory and middle lobes (Fig. 2I). In VAS fetuses, the development of both the left and right domes of the diaphragm was complete (Figs. 2J, K), whereas herniated diaphragm and protrusion of the liver into the pleural cavity was observed in 100% of the late VAD group VI fetuses (Fig. 2L; Table 2). The location of the pericardial membrane suggested that pericardial edema was also a feature in all late VAD fetuses (Fig. 2I). Additional defects that were observed only infrequently in the late VAD group included incomplete development of the interventricular septum, a distal-arising right subclavian aortic arch and an aorta receiving blood from both ventricles in one fetus, and a second had a right-sided aortic arch (data not shown). The low penetrance of these defects suggests that 250 μg atRA/g diet supported aortic arch and septal development and that these processes were completed in the majority of fetuses by E10.5; the two affected fetuses may still have been completing the development of these retinoid-dependent structures when deficiency was imposed after E10.5. This conclusion is supported by the finding that none of these defects were observed in any of the fetuses in the group receiving ROL following the high RA window from E8.5 to 10.5 (group V; Table 2).

Kidney, intestinal, and genital organ development

In all VAS fetuses (groups I, III and V) the kidney was situated normally, posterior to the adrenal gland in the lumbar region of the fetus, and the right and left kidney were separated by the width of the vertebral column (Figs. 2M, N and data not shown). The ureters were dilated (open) normally and ended in the base of the urinary bladder (Figs. 2M and N). In contrast, 100% of late VAD group VI fetuses showed hypoplastic kidneys that were fused at the sagittal midline (horseshoe kidneys; Fig. 2O; Table 2). The renal pelvis and ureter were not open in any of the specimens (Fig. 2O), and the ureter ended in

Table 2
Summary of the defects in the heart, lung, diaphragm, intestine, kidney, ureter and genital tract of late VAD fetuses

	Group						VAD syndrome	Genetic models
	I	III	V	VI	VII	VIII		
Heart abnormalities								
Pericardial edema	6 / 0%	7 / 0%	5 / 0%	1 5 / 100%	7 / 0%	6 / 100%	Yes[a]	Yes[b]
Ventricular septal defect	6 / 0%	7 / 0%	5 / 0%	5 1 / 17%	7 / 0%	5 1 / 17%	Yes[c]	Yes[d]
Lung hypoplasia	6 / 0%	5 2 / 29%	5 / 0%	6 / 100%	7 / 0%	1 2 3 / 83%	Yes[a,e] 4%	Yes[b,d]
Diaphragmatic hernia	6 / 0%	6 1 / 14%	5 / 0%	6 / 100%	7 / 0%	1 5 / 83%	Yes[a,e] 31%	Yes[d]
Intestinal villi hypoplastic	6 / 0%	6 1 / 14%	5 / 0%	1 2 3 / 83%	7 / 0%	1 5 / 83%	NR	NR
Kidney abnormalities								
Hypoplastic kidney	6 / 0%	7 / 0%	5 / 0%	6 / 100%	7 / 0%	7 / 100%	Yes[a]	Yes[b,d]
Kidneys close or fused together	6 / 0%	7 / 0%	5 / 0%	6 / 100%	7 / 0%	1 5 / 83%	Yes[a,e,f] 20%	NR
Ectopia	6 / 0%	7 / 0%	5 / 0%	6 / 100%	7 / 0%	6 / 0%	Yes[e,f] 4%	Yes[b,d]
Pelvis not dilated	6 / 0%	7 / 0%	5 / 0%	6 / 100%	5 2 / 29%	3 3 / 100%	Yes[a,e,f] 36%	Yes[d]
Ureter abnormalities								
Ectopic termination	6 / 0%	7 / 0%	5 / 0%	6 / 100%	7 / 0%	6 / 100%	Yes[e,f] 36%	Yes[d]
Not dilated	6 / 0%	7 / 0%	5 / 0%	6 / 100%	7 / 0%	6 / 100%	Yes[a,f]	Yes[d]
Abnormalities of the genital tract								
Undescended testes	4 / 0%	2 / 0%	3 / 0%	6 / 100%	4 / 0%	1 3 / 75%	Yes[e,f] 54%	NR

Abnormalities are displayed as in Table 1.
[a]Warkany and Roth (1948); [b]Quadro et al. (2005); [c]Wilson and Warkany (1949); [d]Mendelsohn et al. (1994); [e]Wilson et al. (1953); [f]Wilson and Warkany (1948).

the genital ducts instead of the base of the urinary bladder (data not shown). In addition, in all the late VAD group VI fetuses, the fused kidneys were situated ectopically (more caudal) in the lower lumbar/upper pelvic region. Most of the late VAD fetuses also showed less extensive growth of the intestinal villi in the small intestine (compare Fig. 2O to Fig. 2M and Fig. 2N). Genital organ development in the rat is not normally complete until E20.5. Prior to this time (E16–E18), the testes must descend to the pelvic region where they assume their final position in proximity to the urinary bladder. This process occurred normally in the VAS fetuses, whereas the testes failed to descend properly in all male late VAD fetuses (Table 2; compare Fig. 2P and Fig. 2Q to Fig. 2R). Collectively, the work summarized in Tables 1 and 2 and the sections shown in Fig. 2 show that group VI displayed defects with very high penetrance and demonstrate that this dietary approach can be used to produce a defined state of late fetal VAD.

Provision of high dietary atRA from E8.5 to E18.5 results in a partial rescue of the defects observed in the late VAD fetuses

We next sought to determine whether administration of the high atRA (250 μg/g diet) alone from E8.5 onward would support or improve organ development to E18.5. The development of some organs in fetuses receiving the high atRA from E8.5 to E18.5 was clearly improved compared to the late VAD group VI (Tables 1 and 2). In particular, the severity of eye, nasal cavity, lung and kidney defects was significantly reduced in the group receiving prolonged high atRA (group VIII) compared to the late VAD group VI, whereas the development of the diaphragm, ureters and genital organs was improved only slightly or not at all. It is notable that in the group (VIII) receiving the 250 μg atRA/g diet from E10.5 to E18.5, the development of the eye was considerably improved, and the retina was no longer folded although it was somewhat thicker than that seen in the VAS groups (compare Figs. 3B to Figs. 2A and B; Table 1). Nasal cavity development was improved, and the nasal cavity was less severely reduced in size in 83% of fetuses in group VIII compared to VI (compare Fig. 3D and Fig. 2F). Only 50% of the fetuses from group VIII showed severe lung hypoplasia compared to 100% of the late VAD fetuses (group VI; Table 2; compare Fig. 3F to Fig. 2I). In the fetuses exposed to the higher level of atRA to E18.5, the kidneys were no longer fused and were found at the appropriate cranial to caudal position, although they were still situated too close to each other (Fig. 3H). In addition, half of the group VIII fetuses

showed the normal opening of the renal pelvis and the ureter whereas these structures were never open in any of the late VAD fetuses. Importantly, the addition of ROL to the pharmacologic level of atRA (group VII) led to a complete rescue in development of all of these organs. These results show that the pharmacological level of atRA alone improved development, but was not sufficient to meet the total retinoid needs of several organ systems during the latter part of gestation.

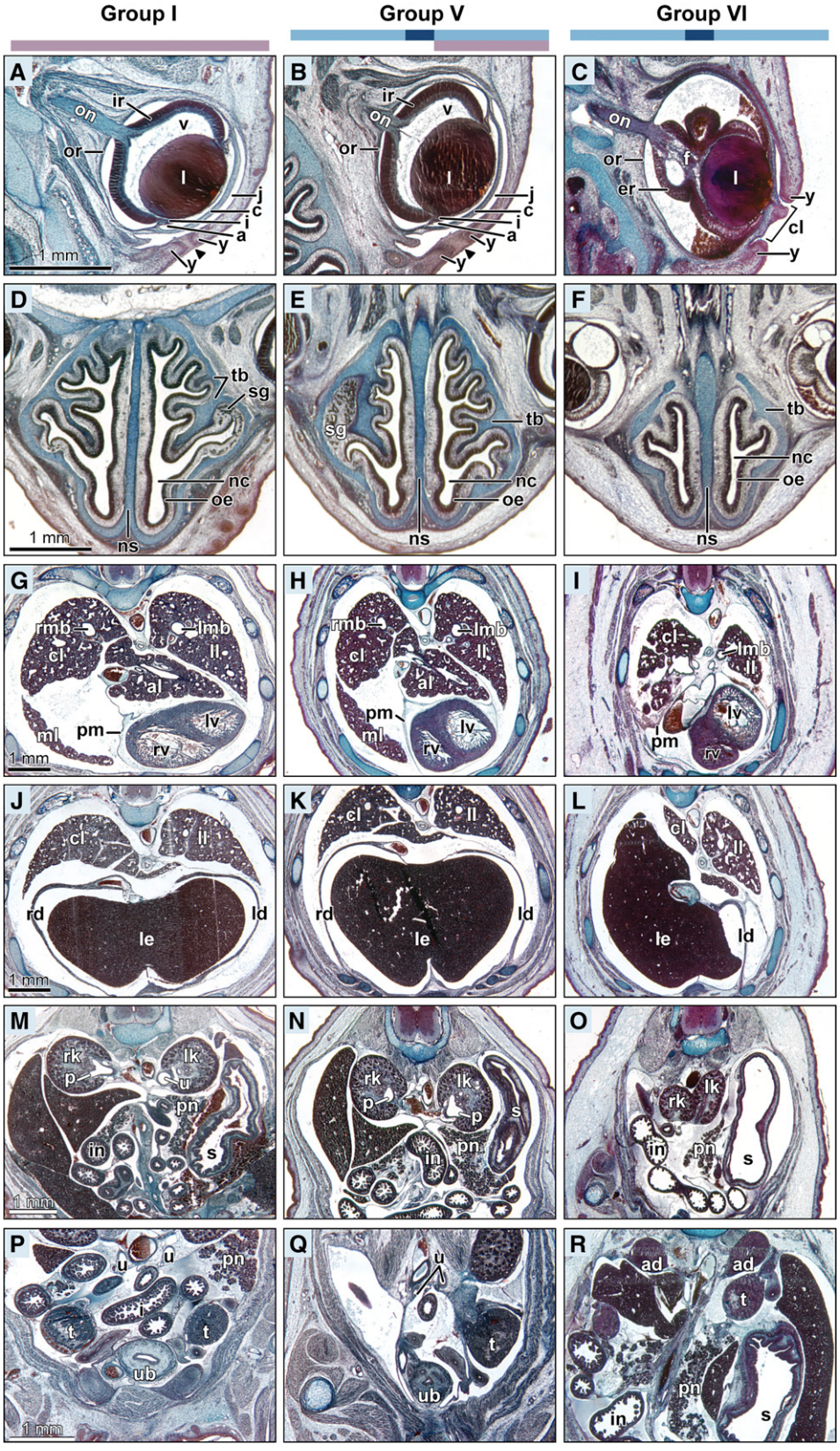

The effect of titrating down the amount of RA on the severity of fetal organ defects

A second study was performed to determine whether reducing the amount of atRA from 12 to 1.5 μg atRA/g diet after E10.5 would further perturb late fetal development (Fig. 4). In this study, fetuses were recovered at E21.5. All fetuses from the VAS control group that received the high amount of atRA from E8.5 to 10.5 followed by supplemental ROL after E10.5 showed normal organ development (group IX, Fig. 4), as did those receiving retinol starting at E0.5 (data not shown). The late VAD group X supplemented with the lower level of atRA (12 μg/g diet) after E10.5 showed developmental defects at E21.5 similar to those observed in the late VAD group VI fetuses examined at E18.5 (compare Figs. 4B, E and H to Figs. 2I, O and F, respectively), however additional defects were also revealed (see below). When the atRA at E10.5 was reduced to 1.5 μg atRA/g diet (group XI), the development of a number of organs including the lung, kidney (Figs. 4C, F), heart and diaphragm (data not shown) was further compromised. Lung hypoplasia was more severe in group XI fetuses (compare Fig. 4C to B). In the 1.5 μg atRA/g diet group (XI), the kidneys were fused, and underwent even more severe hypoplasia than in the 12 μg atRA/g group (compare Fig. 4E and F). Moreover, in the fetuses given the lowest amount of atRA, the kidneys were situated even lower in the pelvic region. Thus, for some organs, reduction of atRA from 12 to 1.5 μg/g diet increased the severity of the VAD-related defects.

Several additional developmental defects were observed in both the 12 and 1.5 μg/g diet groups at E21.5 that were not evident at E18.5. All late VAD fetuses in groups X and XI showed complete Harderian gland agenesis (data not shown). In addition, there was no communication between the nasal and oral cavities (choanal atresia) (Figs. 4H, I), and the maxillary sinus was also missing in both groups of late VAD fetuses.

Imposition of late VAD reveals novel roles for vitamin A in the developing skeleton

Development of the head (cranial region), axial skeleton, pelvis and limbs was examined in group IX, X and XI fetuses at E21.5 of development. As a control for these studies, the VAS group IX fetuses were first compared to those given RP at either E0.5 or E8.5 (Kaiser et al., 2003) and these three groups were found to be normal (Table 3 and data not shown). A similar pattern of defects was observed in both late VAD groups (X and XI); although in some cases, the penetrance was slightly higher in the group receiving the lowest atRA-containing diet. Importantly, the penetrance of most defects approached 100% when the number of fetuses showing any defect (bilateral or unilateral) was considered.

Cranial structures of late VAD fetuses

While imposition of low atRA after the E10.5 stage did not cause gross malformations of the cranial region, it did result in obvious hypoplasia and minor malformation of many of the cranial structures (Fig. 5B). Analysis of the overall length of the dentary, nasal, and incisor bones revealed statistically significant reductions in the late VAD groups compared to the VAS control group (supplemental Table 1), whereas the VAS group did not differ from a control group receiving retinol from the onset of pregnancy (data not shown). The cartilage structures of the nasal turbinates were markedly underdeveloped (Fig. 5D and Table 3), and the supraoccipitals were notably smaller, forming two "islands" as opposed to the normal butterfly shape of this structure (Fig. 5B and data not shown). The medial aspect of the basioccipital was malformed in 83% of the late VAD fetuses in groups X and XI (Fig. 5D and Table 3). Minor malformation or disorganization was seen in the cartilage of the otic capsule; and the bones of the incus, malleus and stapes were present but underdeveloped (data not shown). Notably, the general patterning of the cranial region was preserved in both of the late VAD groups X and XI.

Axial patterning

Late VAD fetuses from groups X and XI showed a sweep of anterior homeotic transformation of vertebral identity from v1/C1 through v10/T3, although not all landmarks were affected (Table 3). This pattern was reversed in the regions of v17/T10, v20/T13, and v27/S1, where evidence of novel posterior homeotic transformations began to appear. The number of presacral vertebra was maintained, with 26 presacral vertebra in 92–100% of the late VAD fetuses despite the many homeotic shifts in identity.

Cervical region

The cervical region of late VAD fetuses from groups X and XI was severely affected, with almost 100% penetrance (Table

Fig. 2. Abnormalities in late VAD group VI fetuses. Transverse sections of E18.5 fetuses showing development of the eye (A–C), nasal region (D–F), lung and heart (G–I), diaphragm (J–L), kidney and intestine (M–O) and male genitalia (P–R). Organ development is normal in the vitamin A-sufficient (VAS) control groups I and V. In the VAD eye (C), note the everted/folded retina (er), open eyelid (bracket), loss of the anterior chamber (a), and fusion of the lens (l) with the cornea (c) forming a corneal–lenticular stalk (cl). The cell free region posterior to the lens or vitreous body (v) is replaced by fibrous tissue (retinolenticular fibroplasia, f). Note the reduction in size of the cartilage primordium of the nasal turbinate bone (tb) and nasal cavity (nc), and loss of the serous gland (sg) in the VAD fetus (F). Note the severe lung hypoplasia and pericardial edema in the late VAD group VI specimen (I). The diaphragm of fetuses in VAS specimens from groups I and V have two complete domes, right (rd) and left (ld) (J, K). In the late VAD specimen (L), the right diaphragmatic dome is not complete. Note the normal position of the right (rk) and left (lk) kidneys in the abdominal region and the openings present in the renal pelvis (p) and ureter (u) in representative VAS specimens (M, N). The late VAD group VI fetus (O) shows fusion of the left and right kidneys that are also hypoplastic and abnormal (pelvic) in location. This specimen also shows less extensive growth of the intestinal villi (in and panels O and R). The testes (t) are positioned normally in the VAS fetuses in groups I and V (P, Q), whereas the testis in the late VAD specimen (R) is situated in the lumbar region instead of lateral to the urinary bladder (ub) in the pelvic region. al, accessory lobe; ad, adrenal gland; cl, caudal lobe; i, iris; in, intestine; ir, neural layer of retina; j, conjunctiva; ll, left lung; lmb, left main bronchus; lv, left ventricle; le, liver; ml, middle lobe; ns, nasal septum; oe, olfactory epithelium; on, optic nerve; or, retinal pigmented epithelium; pm, pericardial membrane; pn, pancreas; rmb, right main bronchus; rv, right ventricle; s, stomach; y, eyelid; filled arrowhead, closed eyelid.

3). While the formation of the hyoid was the least affected, the thyroid, cricoid and tracheal cartilages were severely malformed in 83–100% of the late VAD fetuses, with splitting of the cricoid body and partial to complete loss of the tracheal rings (Table 3 and Fig. 5F). The types of vertebral malformations were consistent across and within litters and represented anterior homeotic transformations of C1 through C7. The C1 vertebra in late VAD fetuses showed dysymphysis of the neural arch, often with a dorsal ossification spot that was either floating or fused to the cranium (Fig. 6B, closed arrowhead, and not shown) in 92–100% of late VAD fetuses. The ventral lamina of C1 attained an exoccipital-like shape (Fig. 6B), and the anterior arch of the atlas (aaa) was fused with the basioccipital (bocc) in the majority of fetuses (Table 3). The neural arches of C2 through C4 were most often fused, and all three vertebrae showed evidence of anterior homeotic transformation, as the dorsal aspect of the lamina took on the shape and characteristics of vertebra further anterior (Table 3 and Fig. 6B, bracket). Although C2 did not show full addition of an ectopic aaa, the dens was fused with the bocc and/or the aaa in the majority of late VAD fetuses, typically by a small cartilage bridge along the dorsal aspect of the aaa (not shown). The neural arch of C3 was split/duplicated (Fig. 6D, filled arrowhead), and the dorsal lamina of vertebra C3 became C2-like in its curvature in 83–100% of the late VAD fetuses in both groups (Fig. 6B). Further posterior, there was evidence of transformation of C7 to C6, as the ventral aspect of C7 gained an abnormally shaped tuberculi anterior, and this structure was lost from C6 also suggesting a C6 to C5 transformation (Fig. 6B).

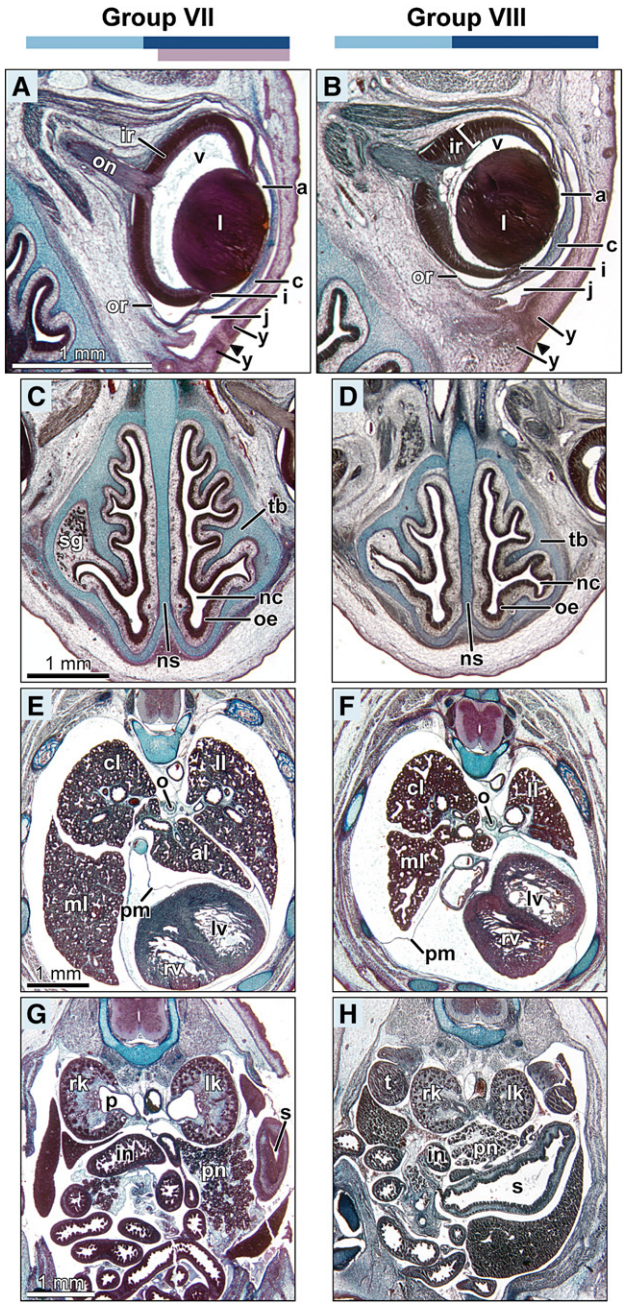

Fig. 3. A pharmacological amount of dietary atRA from E8.5 to E18.5 rescues a subset of the defects observed in fetuses made VAD after E10.5. High atRA (250 μg/g diet) along with ROL starting at E9.5 (group VII, A, C, E and G) resulted in development that was indistinguishable from group I receiving ROL throughout pregnancy (Fig. 2). Eye, nasal, lung and kidney development in the group receiving only the high level of atRA from E8.5 to E18.5 is markedly improved compared to late VAD fetuses (compare Fig. 3B to Fig. 2C; Fig. 3D to Fig. 2F; Fig. 3F to Fig. 2I; and Fig. 3H to Fig. 2O, respectively). In fetuses receiving high RA to the end of pregnancy, the eyelid (y) is closed and the anterior chamber (a) is present (Fig. 3B; Table 1). Note also that the retina in group VIII is curved normally around the lens but appears thickened, particularly in the region nearest the optic nerve (the posterior part of the retina; bracket, B). The development of the nasal region is also improved, however, the serous gland (sg) is still missing (D). The specimen receiving the pharmacological level of atRA from E8.5 to E18.5 shows only mild lung hypoplasia (F). Kidney development is improved as well in group VIII; the two kidneys (rk, lk) are not fused at the sagittal midline as is seen in the late VAD group VI (compare Fig. 3H and Fig. 2O) and the renal pelvis is dilated in half of the group VIII fetuses. Development of the intestinal villi (in) is also improved when the high level of atRA is provided to group VIII. Abbreviations are as in Fig. 2.

Thoracic skeletal elements

Novel anterior and posterior transformations of the thoracic region were observed in the late VAD fetuses. Specifically, v8/T1 and v9/T2 were transformed to a more anterior identity, as evidenced by a partial to complete loss of the v8 ribs and partial loss of v9 ribs in 100% of fetuses examined (Fig. 6D and Table 3). This partial loss of ribs was also seen on v10 in up to 33% of the late VAD fetuses in both groups. Interestingly, the dorsal landmark of vertebral identity on v9, the processus spinosus, was present in its normal location in late VAD fetuses (albeit often smaller than normal; Fig. 6B) while the more ventral identity of this vertebrae appeared to be anteriorized (i.e. partial loss of rib). The sweep of anterior homeotic transformation observed in v8 to v10 ended at some point beyond this axial level, with clear evidence of a reversal or posteriorization events beginning around v17/T10 (dorsal aspect) to v18/T11. In the majority of VAS group IX control fetuses, the dorsal process of the transitional vertebra v18 was flat, curving neither cranially nor caudally (Fig. 6E). In group XI, the dorsal aspect of v18/T11 was curved cranially in 50% of the fetuses, indicating a possible shift to a v19/T12-like identity; and the dorsal aspect of v17/

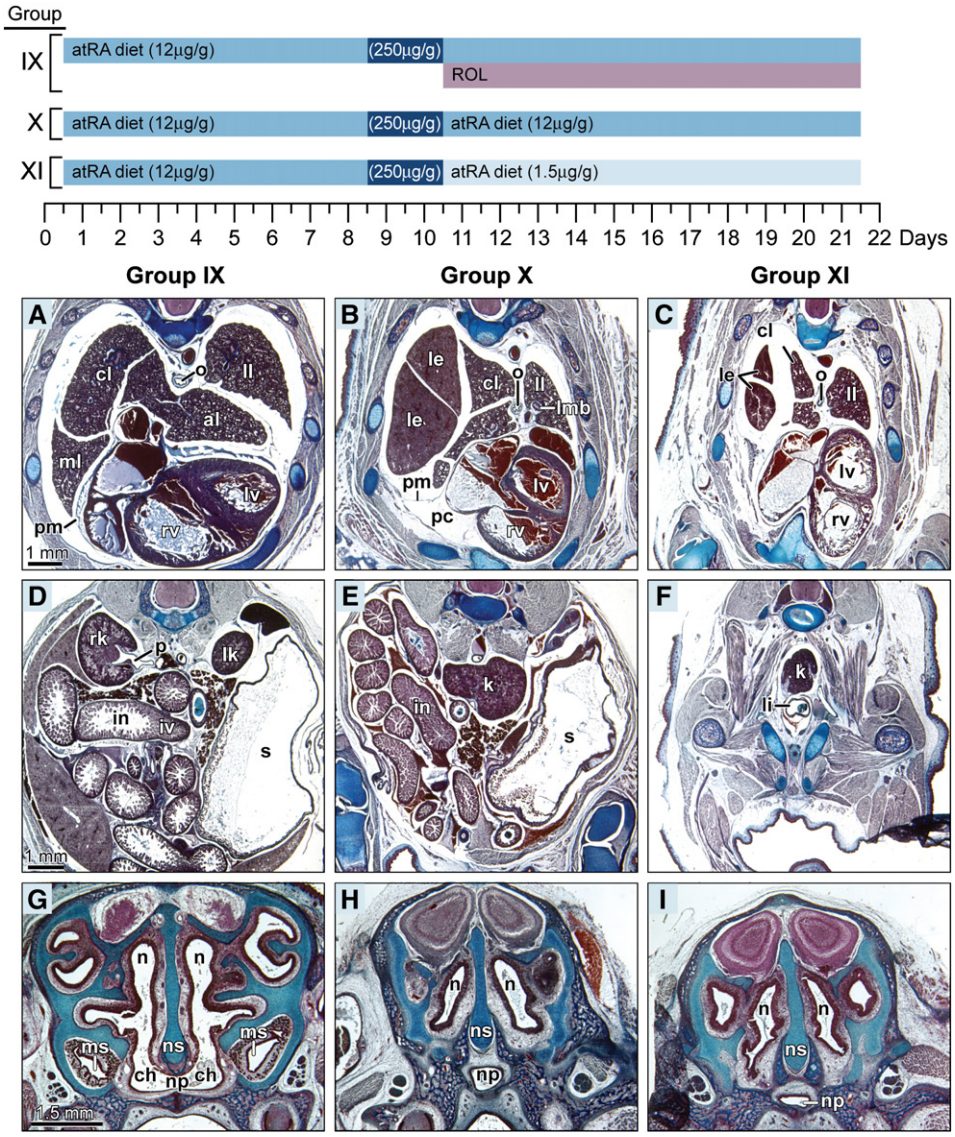

Fig. 4. The effect of reducing material dietary atRA from 12 to 1.5 µg/g diet during the latter part of gestation (E10.5 to E21.5) on fetal organ development. Maternal dietary treatment groups are shown in the top panel. Transverse (A to F) and frontal sections (G to I) are shown. Lung and kidney development is normal in a VAS group IX fetus (A, D). A group X fetus showing hypoplastic lung development (B) similar that seen in the fetuses examined at E18.5 (Fig. 2I). Further reduction of atRA in group XI produces even more severe hypoplasia in all four lobes of the lung (C). Fetus in group X showing fusion of the kidneys (E); group XI fetus with severely hypoplastic fused kidneys located in the lower pelvic region, adjacent to the large intestine (li; F). Nasal region of a VAS fetus with the maxillary sinus (ms) is shown in G, with the choana (ch) connecting the nasal cavity (n) to the nasopharynx (np). Choana is absent (choanal atresia) and agenesis of maxillary sinus is observed in late VAD group X and XI fetuses (H, I). The survival of fetuses at E21.5 in groups X and XI (67% and 66%, respectively) is similar to that of group VI at E18.5. All other abbreviations are as in Fig. 2.

T10 showed a more flattened appearance, suggesting a v18/T11-type shift (Fig. 6F). In addition, 100% of the late VAD fetuses receiving the lowest atRA diet (1.5 µg/g) and 33% in the 12 µg/g group showed a complete loss of the ribs at v20, at least unilaterally, indicating a posterior shift of v20 to a v21-like identity (Table 3 and Fig. 6F). Rib fusions were also observed in the late VAD fetuses, with a high prevalence involving the ribs in the region of v16 through 19, where the majority of fetuses in both groups X and XI (91–100%) showed fusions (Fig. 6D, bracket).

The sternum was grossly malformed in 100% of the late VAD fetuses in both groups (Table 3, Fig. 6H). Only two to four of the thoracic ribs were fused to the sternum and no distinct sternebrae were formed; instead, there appeared to be a fusion of the structures of the manubrium, sternebrae and xyphoid (Fig. 6H, asterisk). Fifty percent of the fetuses in both groups X and XI had a split sternum, with fusion only at the anterior and/or posterior aspect (Fig. 6H and Table 3).

Sacral and pelvic region

Novel malformations were also seen in the sacral and pelvic elements of the late VAD fetuses. There was evidence suggesting a posterior homeotic shift had occurred in the dorsal and ventral cartilage processes of v27/S1 and v28/S2. The

Table 3
Presacral skeletal abnormalities in late VAD fetuses (% of total)

Treatment group	IX (VAS)	X (late VAD)	XI (late VAD)
Retinoid (E10.5-21.5)	ROL	atRA (12 μg/g diet)	atRA (1.5 μg/g diet)
Number of embryos analyzed/number of litters	10/4	12/6	6/3
Cranial and Cervical region			
Hypoplastic nasal turbinates	----	100%	100%
Basioccipital malformed	----	83%	83%
Thyroid cartilage malformed/fused with hyoid	----	83%[a]	100%
Cricoid cartilage malformed/split	----	100%[a]	100%
Two cartilage bands / no tracheal rings	----	91%[a]	100%
C1 - loss of neural arch	----	92%	100%
C1 - dorsal floating/fused ossification body	----	92%	100%
C1 - ventral lamina shaped like exoccipital	----	42% (17%)	67% (33%)
aaa of C1 fused with bocc	----	58%	67%
C2 - neural arch abnormal/fused	----	100%	100%
C2 - ventral lamina C1-like	----	33% (8%)	50%
Dens of C2 fused with bocc and/or aaa	10%	83%	67%
Neural arch fusion occuring C1 through C4	----	92%	100%
C3 - duplication/splitting of neural arch	----	58% (17%)	50% (33%)
C3 - dorsal curvature C2-like	----	83%	100%
C4 - dorsal curvature C2-like	----	17% (8%)	67% (33%)
TA on C6	100%	(42%)	17% (fused)
TA on C7	----	75% (25%)	83% (17%)
Thoracic region			
First full rib on v8/T11	100%	----	----
Complete to partial loss of ribs on v8	----	100%	100%
Partial loss of ribs on v9	----	92% (8%)	100%
Partial loss of ribs on v10	----	16% (16%)	17% (33%)
ps located on v9	100%	100%	100%
Dorsal process v18/T11 flat	80%	92%	50%
Dorsal process v18/T11 curved cranially	----	----	50%
Last full rib on v20	100%	67% (33%)	50% (50%)
Loss of ribs on v20	----	8% (25%)	50% (50%)
Rib fusions v13-v15	----	8% (33%)	17%
Rib fusions v16-v19	----	58% (33%)	83% (17%)
6-7 ribs attached to the sternum	100%	----	----
Only 2 to 3 ribs attached to the sternum	----	83% (17%)	100%
Normal sternum, 4 sternebrae	100%		
Malformed sternum (0-1 sternebrae)	----	100%	100%
Split sternum, fused only anterior/posterior	----	50%	50%
26 presacral vertebrae	100%	92%	100%
27 presacral vertebrae	----	8%	----

Shaded areas indicate normal characteristics. '----': indicates 0% incidence. Percent indicates number of embryos affected bilaterally. Numbers in parentheses denote embryos with only unilateral changes.
C, cervical; T, thoracic; v, vertebra.
[a] $n=11$ analyzed.

dorsal process of v27 lost its characteristic 'half-anvil' shape and became v28-like in shape (Figs. 7B, C, and Table 4). The second sacral vertebra, v28, also had an altered dorsal process that was fused with v27 and/or v29, as well as abnormal ventral processes (Fig. 7E; open arrowhead). All fetuses from both late VAD groups had only 2 or 3 vertebra attached at the pelvis (Table 4 and Fig. 7E). The anterior aspect of the ilial bone was both shortened and malformed, with a widening at the proximal end and no evidence of the sciatic notch (Fig. 7G, compare to Fig. 7F). Moreover, the attachment of the ilium to the spinal column, normally a cartilagenous attachment limited to the medial or inner aspect of the ilium, was markedly deformed. In the late VAD groups, the iliac bone developed a bridge of cartilage curving over the dorsal aspect of the bone and attaching to v27 and v28 (Figs. 7B and C, dashed lines). Fig. 7I demonstrates the very narrowed and abnormal cartilage attachment to the ilium in a late VAD fetus as compared to the control (Fig. 7H), from the dorsal view. This cartilage defect produced an abnormal articulation of the iliosacral joint, with the pelvis and upper hindlimb being rotated ventrally away from its normal alignment with the spinal column in the late VAD groups X and XI (Figs. 7B and C, compare to the VAS control in Fig. 7A).

Limbs

In both late VAD groups (X and XI), the development of both the forelimb and hindlimb was abnormal when compared to VAS control fetuses (group IX). The scapula of the forelimb

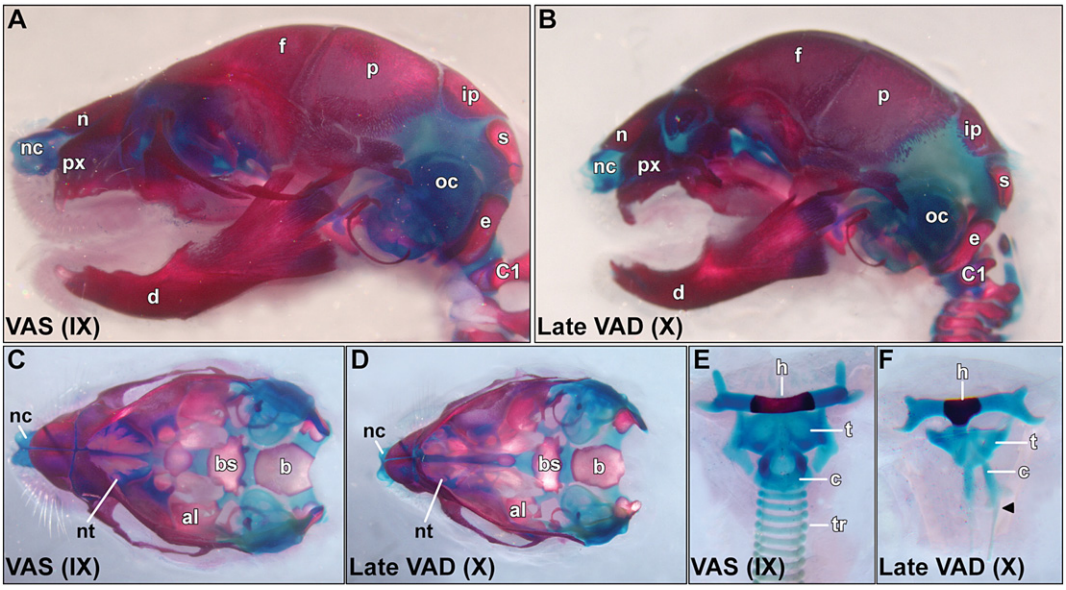

Fig. 5. Comparison of cranial and neck structures in VAS and VAD E21.5 fetuses. Dietary treatment groups are as shown in Fig. 4, top panel. (A) Side view of cranium showing normal development in a control VAS fetus. (B) Group X fetus showing marked hypoplasia of the cranial elements. (C, D) Dorsal view of the ventral cranium, with the dorsal portion of the skull removed. Note the loss of cartilage in the nasal turbinates (nt) and the malformed basioccipital (b) bone in the late VAD fetus shown in panel D. (E) Ventral view of the hyoid (h), thyroid (t), cricoid (c), and tracheal cartilages (tr) showing normal development in a VAS fetus. (F) Late VAD fetus showing gross deformation of the thyroid and cricoid cartilage, and absence of tracheal cartilage rings (closed arrowhead). al, alisphenoid bone; bs, basisphenoid; C1, first cervical vertebra; d, dentary bone; e, exoccipital; f, frontal bone; ip, interparietal bone; nc, nasal capsule; n nasal bone; oc, otic capsule; p, parietal bone; px, incisive bone; s, supraoccipital.

normally has a continuously curved cranial aspect and a straight caudal aspect (Fig. 7J, cranial=top). In both late VAD groups, the proximal end of the cranial edge of the scapula was straight, with the curve beginning about halfway down the length of the bone in 100% of the fetuses examined (Fig. 7K, open arrowhead, and Table 4). Further distal, the normal scapular spine rises higher laterally as it continues distally to form the long flat acromion process (Figs. 7J and L) that articulates with the clavicle and shoulder joint. In almost all late VAD fetuses, the scapular spine appeared hyper-extended laterally, resulting in misdirection of the acromion process and a failure of articulation with the clavicle and shoulder joint (Fig. 7M, double arrowhead and Table 4). The coracoid process, which emanates from the cranial aspect of the articular end of the scapula, normally curves medially in a hooklike shape to articulate with the shoulder joint. In the late VAD fetuses, the coracoid process was somewhat hypoplastic and abnormally rounded (data not shown). The ossification centers of the proximal phalangeal and metacarpal bones were either missing or greatly reduced in size in the distal forelimbs of all group X and XI late VAD fetuses (Fig. 7K and data not shown).

The hindlimb of fetuses from both late VAD groups was abnormal, showing hypoplasia of the proximal fibula, such that normal articulation with the tibia and stifle joint did not occur (compare Fig. 7O to Fig. 7N, and Table 4). Furthermore, as with the thoracic limb, the ossification centers of the proximal phalangeal and metatarsal bones were either missing or severely reduced in size (data not shown).

Thus, both anteriorizations in the cervical and rostral thoracic regions as well as novel posteriorizations in the caudal thoracic and lumbosacral regions of the axial skeleton were revealed in high penetrance in the late VAD fetuses. Overall, there appears to be a need for vitamin A both for early axial patterning as well as for the later development and maintenance of identity for many skeletal elements.

mRNA analysis in late VAD embryos

In order to begin to explore the molecular basis for a number of the skeletal defects appearing in late VAD embryos, studies of *Hoxd3*, *Hoxd4*, *Hoxb4* and *Wnt3a* mRNAs were initiated. While no obvious differences in expression could be detected between VAS and late VAD fetuses for either *Hoxd4* or *Wnt3a* at E11.5 or E12.5, *Hoxd3* mRNA expression was clearly changed in VAD embryos at E11.5. There was a decrease in *Hoxd3* message in VAD group X and XI embryos in the region of pharyngeal arches 3,4 and 6, whereas expression in other areas appeared unchanged from VAS controls (Figs. 8A and B). This is significant, as the third pharyngeal arch contributes to the body of the hyoid bone (lower rim and greater horn) whereas the cartilage of the larynx originates from the fourth and sixth arch mesoderm, and *Hoxd3* plays a role in the formation of these structures (Condie and Capecchi, 1994; Manley and Capecchi, 1997). In contrast, by E12.5, late VAD fetuses showed a clear increase in *Hoxd3* expression and a persistence of signal in the region of somites 22/23, a site where expression was becoming less distinct in the VAS embryos (Fig. 8D and inset). This is interesting, as somites 22/23 contribute to the patterning of vertebra 17 through 19, the region where posteriorization of axial identity begins to become evident in late VAD fetuses. *Hoxb4*, which is needed for proper closure of the ventral body wall as well as normal sternal development (Ramírez-Solis et al., 1993; Barrow and Capecchi, 1996), was

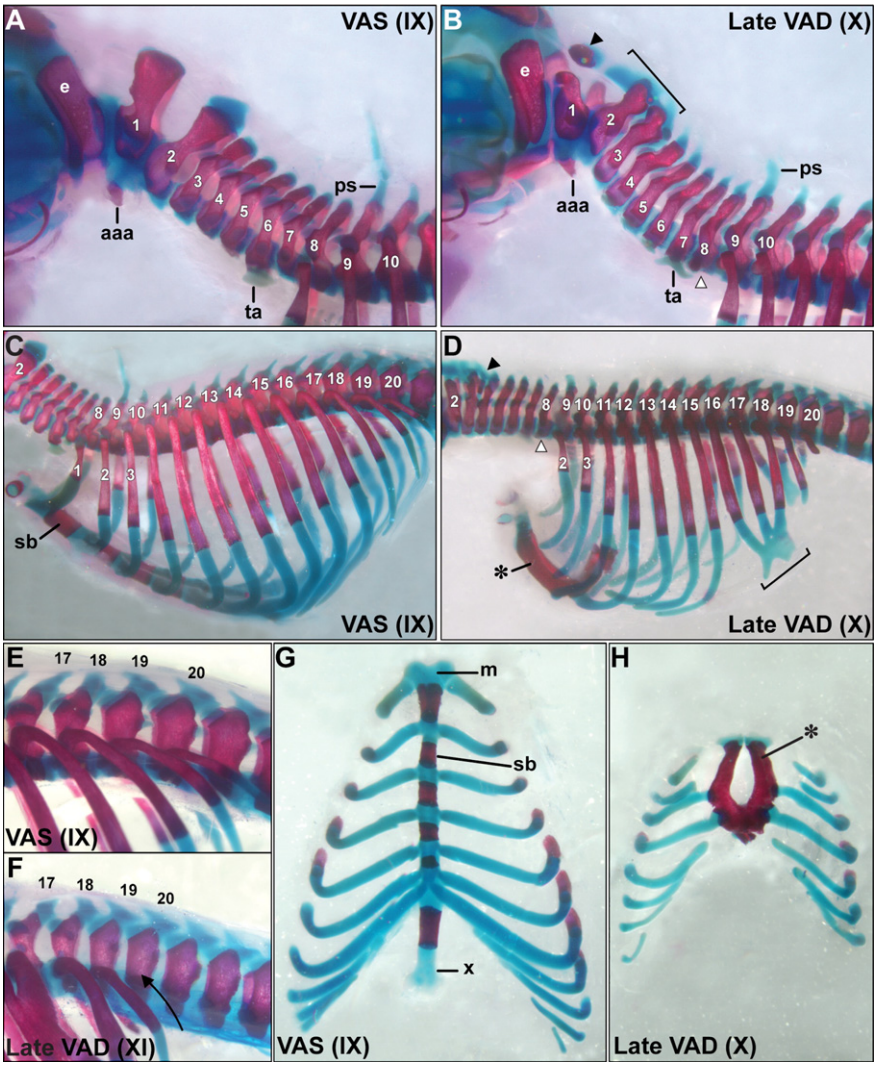

Fig. 6. Homeotic transformations and malformations in the cervical and thoracic regions of late VAD fetuses at E21.5. Numbers indicate vertebra number; in panels C and D, the most anterior ribs are also noted. (A) Side view of cervical region showing normal skeletal elements in a VAS fetus. (B) Late VAD fetus showing fusion of the cervical arches of v1–v3 (bracket) and anteriorization of v7 (tuberculi anterior, ta, on C7) and v8 (loss of rib, open arrowhead). The closed arrowhead in panel B indicates a floating ossification body above C1. (C) Side view of the thoracic region showing normal development in a group IX fetus. (D) Late VAD fetus showing anteriorization and posteriorization events in the thoracic region. Note rib fusions on v16–v18 (bracket), loss of rib on v8 (open arrowhead, anteriorization) and partial loss of the rib on v20 (posteriorization), and sternal malformation (asterisk). (E) Close view of vertebra in the transitional region of the thoracic spinal column (v17 through 20), showing the normal flattened dorsal process on v18 and rib on v20. (F) Late VAD fetus with posteriorization of the dorsal process of v17/v18 and loss of the rib on v20 (curved arrow). (G) Ventral view of the sternum showing normal development of the manubrium (m), sternebrae (sb), xyphoid process (x) and ribs in a VAS fetus. (H) Late VAD fetus showing gross malformation of the sternal elements as well as loss of ribs attached to the sternum. The asterisks in panels D and H indicate fusion of the manubrium, sternebrae and xyphoid process in late VAD fetuses. aaa, anterior arch of the atlas; e, exoccipital; ps, processus spinosus.

also decreased in late VAD embryos at E16.5 in the region medial to the cartilage primordium of the sternum (Fig. 8F), whereas it was expressed at a similar level to that of the VAS controls in the spinal cord (Figs. 8E and F; insets). These preliminary findings suggest that changes in expression of at least two *Hox* gene family members (*Hoxd3* and *Hoxb4*) could play a role in the skeletal changes that result from imposing VAD after E10.5 in the rat, although there are likely to be many other gene changes that contribute due to the pleiotropic nature of atRA action. The reduction in *Hoxd3* expression that is observed in late VAD embryos at E11.5 also suggests that a state of VAD is imposed in embryos very rapidly (within 24 hours) after reducing the maternal dietary intake of atRA, and is in agreement with the short half-life of the vitamin A acid reported *in vivo* (Roberts and DeLuca, 1967).

Discussion

Nutritional approaches have been used successfully to evaluate the need for vitamin A early in mammalian embryogenesis, whereas the ability to induce VAD at later times has been hampered by the high lethality that occurs when retinoid is limiting. In this paper, a nutritional model is described that produces vitamin A deficiency in rat fetuses during later gestation (late VAD). This is achieved by supplying atRA in the diet to pregnant VAD female rats, first at a low level, and then at

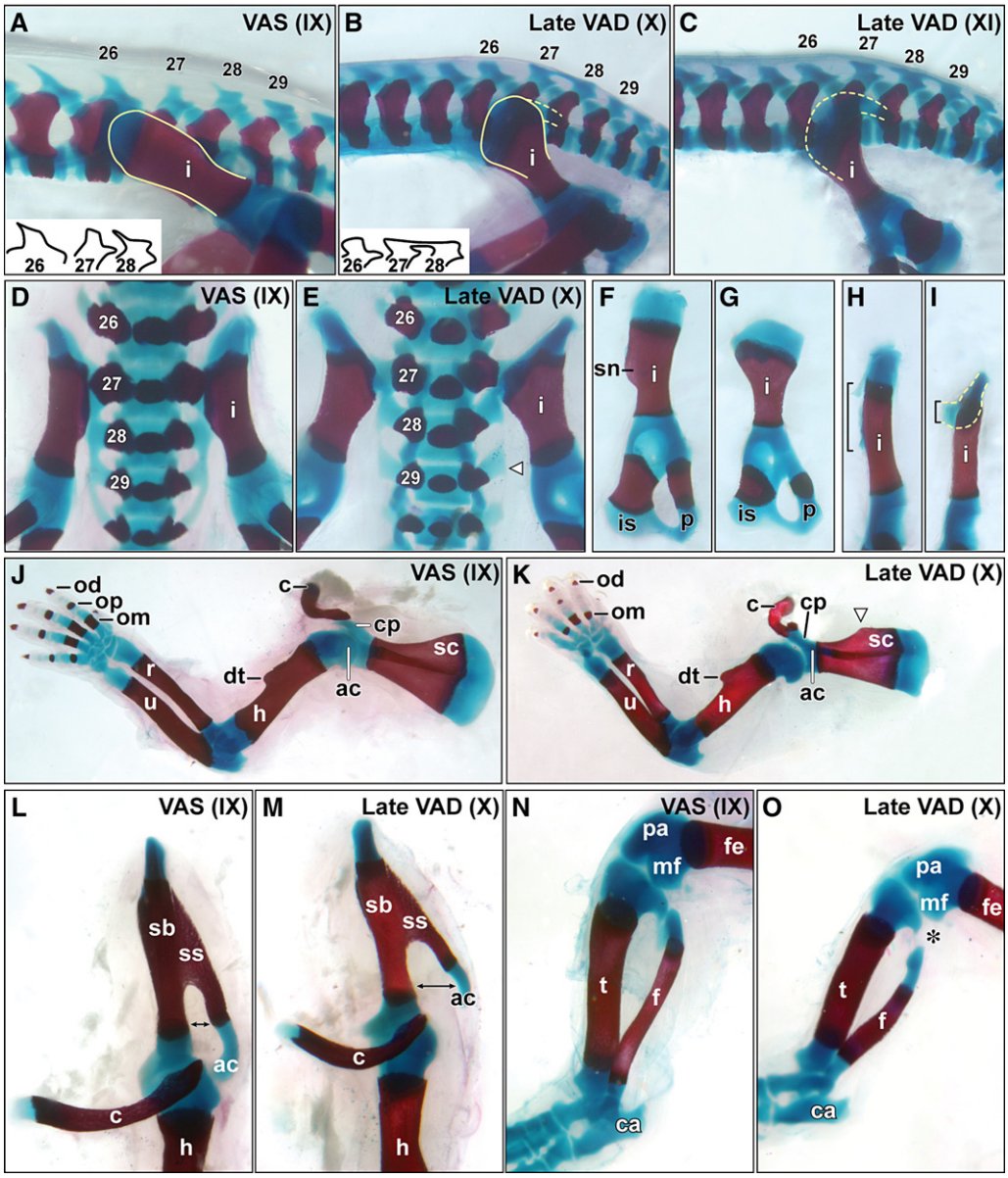

Fig. 7. Malformations in the pelvic and sacral regions, and in limbs of VAS and VAD fetuses at E21.5. Numbers indicate vertebra number. (A) Side view of sacral region of a VAS fetus depicting normal development and attachment of the ilium (i; solid outline) and characteristic shape of the dorsal processes of v26–v29. (B) Late VAD (group X) fetus showing moderately abnormal attachment of the ilium and widened anterior ilium (dotted outline indicates abnormal bridge of dorsal cartilage to v27/v28) as well as posteriorization of the dorsal processes of v26 and v27. (C) Group XI fetus showing severely abnormal ilium and attachment at sacrum (dotted line indicates abnormal dorsal cartilage attachment) and posteriorization events in v26–v28. (D) Ventral view of the sacrum of a VAS group IX fetus showing normal pelvic and sacral development. (E) Ventral view of late VAD fetus with marked deformation of the sacral attachment and abnormal lateral processes of v28 and v29 (arrow). (F) Medial (inner) view of the ilium of a control fetus showing normal shape of the ilium and sciatic notch (sn). (G) Ilium of a group X fetus with shortened, widened anterior aspect of ilium and loss of the sciatic notch. (H) Dorsal view of ilium (medial to left, lateral to right) of a VAS control fetus. Brackets indicate the area where the normal cartilage attachment to the sacral vertebra is located on the medial (inside) aspect of the bone. (I) Dorsal view of ilium of a group X late VAD fetus showing the abnormal dorsal cartilage that bridges to the sacral vertebra. Late VAD fetus showing hypoplastic forelimb (K, M) and hindlimb (O) when compared with VAS fetus (J, L, N). Note the abnormal shape of the cranial border of the scapula in the late VAD fetus (K; open arrowhead) whereas it is concave in shape in the VAS fetus (J). In the VAS fetus, the spine of the scapula (ss) articulates to the humerus (h) and to the clavicle (c) through the acromion process at the acromioclavicular joint as shown in panel L, which shows side view of the scapula blade (sb). In the late VAD fetus, the spine of scapula and the acromion are hyperextended and project further away from the scapular blade than normal (M; double arrow). Close-ups of hindlimbs are shown in panels N and O. The fibula (f) articulates to the femur (fe) in the VAS fetus (N), whereas in late VAD fetus, the fibula is hypoplastic and does not form the tibiofibular articulation (asterisk, F). ca, calcaneum; cp, coracoid process; dt, deltoid tuberosity; i, ilium; is, ischium; mf, medial fabella; od, ossification center in distal phalangeal bones; om, ossification center in metacarpal bone; op, ossification center in proximal phalangeal bone; pa, patella; p, pubis; r, radius; sc, scapula; t, tibia; u, ulna.

a higher level (250 μg atRA/g diet) during a time that corresponds to the late gastrula/early neurula stage to around the 12–15 somite stage. When a diet containing a lower level of atRA is reinstituted after E10.5, a well-defined state of vitamin A deficiency is produced revealing defects in organogenesis and skeletal development (Tables 1 and 2). A subset of the defects

Table 4
Sacral and limb abnormalities in late VAD fetuses (% of total)

Treatment group	IX (VAS)	X (late VAD)	XI (late VAD)
Retinoid (E10.5-21.5)	ROL	atRA (12 μg/g diet)	atRA (1.5 μg/g diet)
Number of embryos analyzed/number of litters	10/4	12/6	6/3
Sacral region			
Normal ilium (anterior width)	100%	----	----
Normal iliosacral articulation	100%	----	----
Widened anterior ilium	----	100%	100%
Abnormal iliosacral angle	----	100%	100%
Dorsal v27 'half-anvil'	100%	----	----
Dorsal v28 'full-anvil'	100%	----	----
Dorsal v27 to v28-like	----	100%	100%
Dorsal fusions v27-v30	----	100%	100%
4 vertebrae attached at pelvis	100%	----	----
3 vertebrae attached at pelvis	----	50% (17%)	33% (50%)
2 vertebrae attached at pelvis	----	33% (17%)	17% (50%)
Forelimb			
Abnormal curvature to cranial aspect of scapula	----	100%	100%
Misdirection of acromion process	----	67% (17%)	83% (17%)
Malformed coracoid process	----	75% (17%)	100%
Hindlimb			
Hypoplasia of proximal fibula	----	100%	83% (17%)

Shaded areas indicate normal characteristics. Percent indicates number of embryos affected bilaterally. Numbers in parentheses denote embryos with only unilateral changes.
v, vertebra.

produced in this late VAD model are similar to those described in the 1940s and 50s coined the "vitamin A deficiency syndrome" (Warkany and Schraffenberger, 1944, 1946; Jackson and Kinsey, 1946; Warkany and Roth, 1948; Warkany et al., 1948; Wilson and Warkany, 1949; Wilson et al., 1953). However, in these early studies, the time to depletion and the severity of the deficiency varied, the maternal and fetal survival rates were low, and the non-eye-related defects were observed only at low frequency (4–42%). Using the late VAD model described here, not only do fetuses recapitulate most of the defects described in these early studies, but the maternal and fetal survival rates are much higher, and malformations are observed in nearly 100% of the fetuses. The key methodological improvement involves the use of the short half-life vitamin A metabolite, atRA, thus enabling provision of an exact amount of the retinoid at appropriate times in a form that cannot be stored.

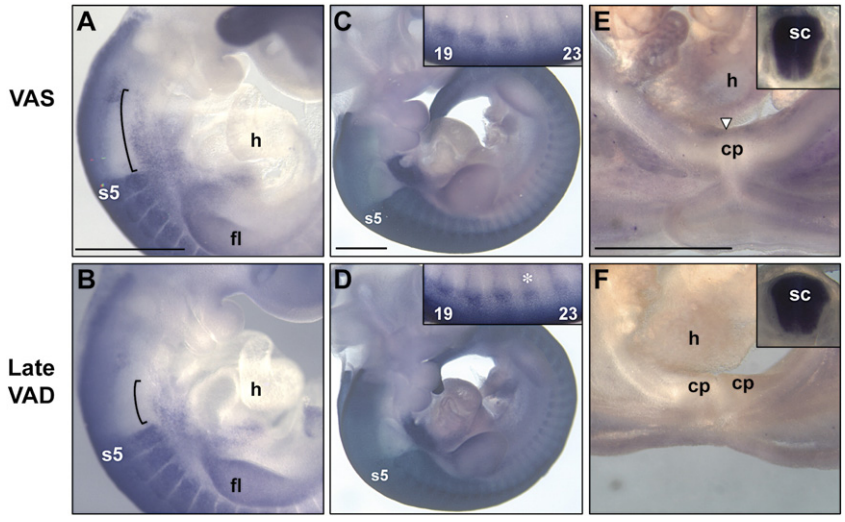

Fig. 8. *Hoxd3* and *Hoxb4* mRNA expression in late VAD compared to VAS embryos. (A) Normal expression of *Hoxd3* mRNA is seen in a VAS embryo at E11.5 (B). Note the decrease in *Hoxd3* expression in the region of pharyngeal arches 3, 4 and 6 (bracket). *Hoxd3* staining in a VAS control (C) and late VAD (D) embryo at E12.5. The inset shows the slight increase in punctate dorsal staining in the region of somites 22 (asterisk) and 23 in the late VAD embryo compared to the control. Vibratome sections showing *Hoxb4* expression in a VAS control embryo at E16.5 (E) and the reduction in staining in the late VAD embryo. Equivalent staining is shown in the spinal cord (insert) for comparison. cp, cartilage primordium; fl, forelimb; h, heart; s, somite; sc, spinal cord.

Importantly, the cardiac defects that may have contributed to high embryonic lethality in earlier studies are avoided in the present model. Using this model, a defined state of fetal VAD is attained, and the severity of defects in some tissues (lung, kidney, heart and diaphragm) can be further modulated by titrating the level of atRA included in the diet. This model can now be extended to study the effects of VAD at specific times during later development by varying the time when retinoid is added back to the diet.

VAD syndrome-like defects have been reported in compound, but not single, RAR null mutants, and it is noteworthy that the penetrance of many of these defects is often quite low (Lohnes et al., 1994; Mendelsohn et al., 1994; Grondona et al., 1996). *RARα*$^{-/-}$*RARγ*$^{-/-}$ fetuses showed the highest penetrance, however, there was a high embryonic mortality rate (Lohnes et al., 1994). *Raldh* null mutants have also been used to study the function of RA in developing embryos, but this approach is complicated by the presence of multiple RALDH enzymes (Duester et al., 2003; Dupe et al., 2003; Fan et al., 2003; Matt et al., 2005; Molotkov et al., 2006) as well as a newly described Cyp1B1 (Chambers et al., 2007), all of which may contribute to the atRA that is present at varying times during the development of the embryo. atRA supplementation of mothers of *Raldh2* null mutants has been shown to extend survival to later times (E18.5), but only a very small number of mutants were rescued (2 fetuses out of 12 litters) (Wang et al., 2006). Thus, the late VAD rat model described here represents a means whereby the developmental effects of deficiency can be studied in a model with high fetal survival and penetrance of defects.

In addition to recapitulating many of the defects described by Warkany and colleagues, the late VAD model has revealed malformations not observed in these early studies. In some cases, these late VAD defects show similarity to those observed when a genetic approach is used to alter retinoid signaling. Specifically, the choanal atresia observed in *Raldh3*$^{-/-}$ fetuses, absence of salivary glands in *RAR* compound mutants (Lohnes et al., 1994), and agenesis of the Harderian glands found in *RAR* compound mutants, *Raldh3*$^{-/-}$ (Dupe et al., 2003) and *Raldh1*$^{-/-}$*Raldh3*$^{-/-}$ mutants (Matt et al., 2005) are also seen in late VAD rat fetuses. Nasal cavity development begins in the mouse at E9.5 (11–11.5 in the rat), and the timing of late VAD coincides with a time when an effect on this structure would be expected. The present work proves that a lack of vitamin A is clearly the precipitating event leading to these defects, as opposed to the involvement of RALDH or RAR in other metabolic or signaling pathways. Thus, these embryonic defects can now also be considered part of the VAD syndrome.

In the present model, because VAD is imposed after E10.5 (~12–15 somite stage), the late VAD fetuses differ somewhat with respect to lung and heart changes when compared to those reported as part of the early VAD syndrome and in genetic models that alter retinoid signaling during all stages of embryonic development. In late VAD rat fetuses, the lungs are hypoplastic, but no agenesis is observed. In contrast, left lung agenesis and lung hypoplasia was reported by Warkany and colleagues (1948) and Wilson et al. (1953), and was also observed in *RAR* compound mutants (Mendelsohn et al., 1994), *RBP* (Quadro et al., 2005) and *Raldh2* mutants supplemented with RA (Wang et al., 2006). Lung development starts at approximately E10.5 in rat embryos (E9 in mouse; Maeda et al., 2007) and the lung buds arise from the foregut endoderm followed by branching of the bronchial tree starting at approximately E13 in rats (E11.5 in mouse; Kaufman, 1992). Lung agenesis may have resulted from disruption in retinoid signaling during lung bud formation, whereas, in the late VAD model, the pharmacological level of atRA (250 μg atRA/g diet) provided from E8.5 to E10.5 supported budding of lung from the foregut. However, the low atRA diet (12 μg atRA/g diet) after E10.5 was clearly insufficient to support the branching and growth of the lung that happens during later gestation yielding hypoplasia.

Cardiac and aortic arch defects were infrequently observed in late VAD fetuses in the present study when compared to other models (Wilson and Warkany, 1949; Mendelsohn et al., 1994). The heart is the first organ to develop in the embryo, starting at approximately E7–7.5 in the mouse (E9–9.5 in rat) when the intra-embryonic mesoderm splits to form the intra-embryonic coelom (Kaufman, 1992). The pericardial coelom continues to develop and by E8–8.5 in the mouse (E10–10.5 in rat), the cardiac primordium is undergoing looping and the primitive vasculature is established. The pharmacological amount of atRA consumed by dams during midgestation prevented the majority of the cardiac and aortic arch defects from occurring in the majority of late VAD fetuses. Thus, the model presented here can be used to address the importance of timing of retinoid sufficiency in relationship to the development of specific embryonic structures without significant lethality due to disruption of heart development.

Although much of skeletal patterning is initiated early in development, the process of chondrocyte migration, differentiation and subsequent ossification occurs later. Skeletal staining of late VAD fetuses reveals novel malformations of both axial and appendicular skeletal elements, including homeotic transformations that include both anteriorizations and posteriorizations at different axial levels in the same fetus. Using a nutritional approach to impose VAD at earlier times during rat embryonic development (<E10.5), our group showed previously that vitamin A plays a critical early role in patterning the entire axial skeleton (Kaiser et al., 2003). The present study now clearly demonstrates that vitamin A also plays key roles at later times in the maintenance of vertebral identity and in the development other structures. Interestingly, skeletal abnormalities were not originally reported as part of the VAD syndrome, but they were reported in the cranial and cervical regions of *RAR* single (Lohnes et al., 1993) and compound (Lohnes et al., 1994) null mutant mice. Thus, our work shows that skeletal abnormalities should be added to the VAD syndrome, and confirm the necessity for ligand in these processes. Because the late VAD model also produces novel malformations, it either must represent the most severe dampening of vitamin A signaling produced to date, and/or shows that a loss of ligand-dependent repressive function impacts development more severely than does the absence of receptors. The importance

of ligand-dependent repression has been clearly documented in the thyroid hormone field, where the effect of thyroid hormone deficiency is more severe than the loss of thyroid hormone receptors (Eckey et al., 2003).

Comparison of the effects of early and late VAD to the defects observed in genetic models that perturb vitamin A signaling also now enables us to define when during development vitamin A-dependent processes are altered. Several regions of the late VAD skeleton are less severely affected than in genetic models that interfere with vitamin A signaling for the entire course of embryogenesis. In the craniofacial region, the loss of midfacial structures seen in $RAR\alpha^{-/-}RAR\gamma^{-/-}$ compound (Lohnes et al., 1994) or *RBP* (Quadro et al., 2005) knockout models is not observed the late VAD fetuses presented here. Likewise, in late VAD fetuses, the most distal regions of the forelimb and hindlimb are somewhat hypoplastic, but overall, these appendages are patterned appropriately. This contrasts with the $RAR\alpha^{-/-}RAR\gamma^{-/-}$ mutants, where ectrodactayly and polydactyly are observed (Lohnes et al., 1994). This shows that provision of an amount of atRA that supports normal growth and cellular differentiation in the adult (12 μg atRA/g diet) to E8.5 followed by higher RA to 10.5 is sufficient to support early patterning and development of facial structures and distal regions of the limb in the embryo.

There are similarities between fetal defects induced by the late VAD model and compound RAR null mutant mice, particularly in the upper cervical regions of the skeleton. Late VAD causes a high penetrance of defects of the thyroid, cricoid and tracheal cartilages, similar that reported in $RAR\alpha^{-/-}RAR\gamma^{-/-}$ mutants (Mendelsohn et al., 1994) whereas these defects are not seen in early VAD. Interestingly, imposition of VAD after E10.5 resulted in down-regulation of *Hoxd3* at E11.5 in the caudal pharyngeal arches (3, 4 and 6). These regions contribute to the hyoid and laryngeal cartilages, and deletion of *Hoxd3* has been shown to enhance the *Hoxa3* mutant phenotype in the laryngeal cartilages (Condie and Capecchi, 1994), and *Hoxd3/Hoxb3* double mutants show defects in the throat cartilages and bones that are not seen by mutation of either individual gene (Manley and Capecchi, 1997). Deformation of C1 was reported in $RAR\alpha^{-/-}RAR\gamma^{-/-}$ mutants and is also seen when VAD is imposed either early or late; however the VAD phenotypes vary depending upon the timing of the deficiency. Early VAD (E9.25–E9.75) causes a posterior shift in the expression of *Hoxd3* and *Hoxd4* in the somitic mesoderm and anteriorization of C1 and C2 (Kaiser et al., 2003), whereas this shift in *Hox* gene expression was not observed in late VAD embryos (Fig. 8 and data not shown). Interestingly, marked agenesis of the neural arch of C1 is not seen with high penetrance in early rescued VAD fetuses, but is found with very high penetrance (92–100%) in late VAD fetuses in the present report. It is only in late VAD fetuses that formation of an ectopic bone element in the dorsal cervical region of C1 is observed. The malformations due to late VAD in this region are strikingly similar to those reported by Lohnes and colleagues (1994) in $RAR\alpha^{-/-}RAR\gamma^{-/-}$ mutants, in which both agenesis of the C1 neural arch and ectopic bone elements in the cervical region were noted. The fact that tracheal defects do not occur and ectopic bone in the region is not found unless deficiency is imposed after E10.5 would indicate that it is not only signaling through the RARs, but signaling beyond the 12 to 15 somite stage that is crucial.

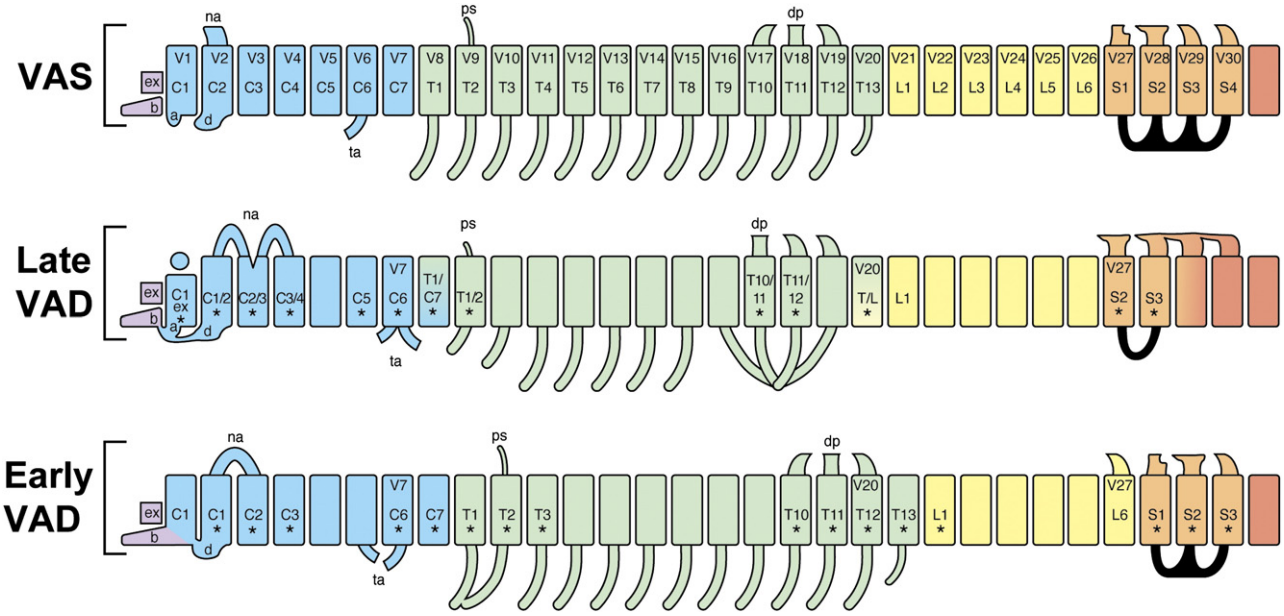

Fig. 9. Schematic summarizing how vitamin A deficiency imposed at different times during development alters vertebral development and axial patterning. Late vitamin A deficiency (deficiency > E10.5; groups X and XI) leads to both anterior and posterior vertebral transformations, whereas fetuses deficient in retinoid at earlier developmental times (between E9.25 and 9.75) show only anteriorizations extending from v1 to v30 (adapted from Kaiser et al., 2003 and unpublished observations). Fetuses showing normal development (VAS) include those given retinol at E0.5, or those fed a diet containing 12 μg atRA/g diet and either supplemented with 250 μg atRA/g diet (E8.5–E10.5) followed by retinol at E10.5 (group IX) or supplemented with retinol before E9.25 (Kaiser et al., 2003). a, anterior arch of the atlas; b, basioccipital; d, dens; dp, dorsal process; ex, exoccipital; na, neural arch; ps, processus spinosus; ta, tuberculum anterior; v, vertebra. C, cervical; T, thoracic; L, lumbar; S, sacral. ∗indicates transformation to a different vertebral identity.

One of the most surprising findings is that late VAD fetuses show both anterior and posterior homeotic axial skeletal transformations. This is in striking contrast to the effect of early VAD that results in a sweep of anteriorization extending from v1 to v30 (Fig. 9). The importance of atRA as a posteriorizing factor in the cervical region of the axial skeleton has been demonstrated both in fetuses made VAD prior to E10.5 (Kaiser et al., 2003) and in genetic models in which RARs are disrupted (Lohnes et al., 1993; 1994). Interestingly, both in the cervical region (C2–C7) and at the cervical/thoracic junction of late VAD fetuses, homeotic shifts representing anteriorizations are observed. The anteriorizations produced by late VAD are, however, completely prevented when high atRA is given from E8.5 to E10.5 followed by retinol, showing that it is VAD after E10.5 that is responsible for the malformations seen in the present study. The presence of RARα and γ transcripts in sclerotomes of the mouse (Ruberte et al., 1990, 1991; Dolle et al., 1990) supports the idea that atRA may act directly in this tissue to support later maintenance of vertebral identity. At the thoracic junction, the late VAD model continues to yield anteriorization events, as evidenced by the loss of ribs at v8 and the presence of partial ribs at v9, with 100% penetrance. However, the dorsal landmark of identity on v9, the processus spinosus, is in place, indicating a differential effect of late VAD on the dorsal and ventral identity of v9. These late VAD-induced changes contrast with those of $RAR\alpha^{-/-}RAR\gamma^{-/-}$ compound knockouts in which posterior transformations occur at this junction, with the addition of ribs on C6 and C7 (Lohnes et al., 1994). The VAD fetuses do, however, reveal two very striking novel posteriorization events in more caudal regions of the skeleton. Vertebra 17 through 20 (T10–T13) appear posteriorized, as evidenced by the change in the transitional vertebra shown and the loss of a rib on v20 shown in Fig. 6F. Although these defects have not been reported in any genetic models that disrupt vitamin A signaling, similar defects have been reported by Ikeya and Takada (2001) in *Wnt-3a*$^{vt/vt}$ mutant mice, in which posteriorization of the transitional vertebra (dorsal aspect) and loss of the ribs on v20 is reported. We could not detect any changes in Wnt3a expression in late VAD embryos at either E11.5 or E12.5. However, we did observe higher levels of *Hoxd3* expression at E12.5 in late VAD embryos in this key region (somites 22/23). These somites contribute to v17–v19, and correspond to the region where we see posteriorization of the dorsal neural arches and a loss of the rib on v20. It is possible that aberrant persistence of *Hoxd3* expression in this region could contribute to the mispatterning (posteriorization) in the late VAD groups, or at least indicates that there is aberrant gene expression that results from late VAD in this region. Further caudal in VAD fetuses, the dorsal processes of sacral v27 and v28 both show evidence of posteriorization. These more posterior homeotic transformations are in clear contrast with the $RAR\alpha^{-/-}RAR\gamma^{-/-}$ mutant, in which no homeotic changes beyond the cervical/thoracic junction are reported. Because late VAD embryos are devoid of all vitamin A except that provided in the form of atRA to the maternal organism, the patterning effects in our model may represent a more complete impairment of vitamin A signaling compared to the situation when only two RAR subtypes are missing yet the retinoid biosynthetic machinery remains intact.

In addition to changes in axial patterning, dramatic malformation of the sternum and ribs occur due to late but not early VAD (on or before E9.75; Kaiser and Clagett-Dame, unpublished observations). Sternal development begins around E12 in the mouse (Chen, 1952), therefore it is not surprising that the development of this structure is strongly affected only when VAD is imposed at later times (Table 5). The sternal deformations seen here are more severe than those observed in genetic models that perturb vitamin A signaling (Lohnes et al., 1994; Quadro et al., 2005). Not only are the sternal bands not fused in late VAD fetuses, but there is a complete absence of the non-ossified regions that normally separate the sternebrae. Split sterum and sternal malformations have been reported in *Hoxb2* and *Hoxb4* single as well as *Alx4/Cart1* double homozygous

Table 5
Comparison of skeletal defects in late VAD fetuses with early VAD and genetic models that affect retinoid signaling

	Late VAD (>E10.5)[a]	Genetic models	Early VAD[b] (E9.25–9.75)[a]
Craniofacial skeleton			
Loss of midfacial structures	No	Yes[c,d]	No[e]
Hypoplastic cranial bones	Yes	Yes[c,d]	No
Thyroid and cricoid cartilages abnormal	Yes	Yes[f]	No[e]
Tracheal rings lost	Yes	Yes[f]	No[e]
Axial skeleton			
Homeotic transformations			
Basioccipital with aaa fusion	Yes	Yes[c,g]	Yes
Anteriorization of C1/C2 lamina	Yes	Yes[c,g]	Yes
Anteriorization of C7 to C6 (ta on C7)	Yes	Yes[c,g]	Yes
Posteriorization C7 to T1 (rib on C7)	No	Yes[c]	No
Anteriorization of T1/T2 (rib loss v8/v9)	Yes	NR	Yes
Posteriorization of v17/v18 to v18/v19	Yes	NR	No
Posteriorization T13 to L1 (rib loss v20)	Yes	NR	No
Posteriorization v26/v27 to v28/v29	Yes	NR	No
Malformations			
Loss of C1 neural arch	Yes	Yes[c,d]	Yes
Ectopic bone in dorsal cervical region	Yes	Yes[c]	No
Loss of C2 neural arch	Yes	Yes[c]	No
Rib fusions v8 and v9	Yes	Yes[g]	Yes
Rib fusions v13–15/v16–19	Yes	NR	No
Sternal splitting and loss of sternebrae	Yes	Yes[c,d]	No[e]
Iliosacral joint malformation	Yes	NR	No

NR, not reported.
[a] Time when embryos were retinoid-deficient.
[b] Kaiser et al. (2003).
[c] Lohnes et al. (1994).
[d] Quadro et al. (2005).
[e] Kaiser and Clagett-Dame, unpublished observations.
[f] Mendelsohn et al. (1994).
[g] Lohnes et al. (1993).

mice (Ramírez-Solis et al., 1993; Barrow and Capecchi, 1996; Qu et al., 1999). The loss of *Hoxb4* expression noted in the ventral body wall adjacent to the cartilage primordium in late VAD embryos may have contributed to the sternal malformations observed in this group. The *Hox* genes are believed to play an indirect role in closure of the sternal rudiments, and are known to be regulated by atRA (Ramírez-Solis et al., 1993; Roelen et al., 2002). In addition, ventral rib fusions from v16 to v19 are seen with high frequency in late VAD, and may be similar to those observed in $RAR\alpha^{-/-}RAR\gamma^{-/-}$ nulls (Table 5).

Novel and highly penetrant malformations of the pectoral and pelvic regions are apparent in late VAD rat fetuses. In the pectoral region, the acromion process is misdirected, and the proximal region of the scapula is malformed. In the pelvic region, there is an abnormal cartilage connection extending from the ilium causing an aberrant rotation of the hindlimb away from the spinal column. The scapula and ilium are the dorsal components of the shoulder and pelvic girdles. Although the pathways responsible for the formation of these structures are not well understood, *Emx2* is known to be essential for the formation of structures of both girdles (Pellegrini et al., 2001), *Tbx15* and *Alx4* play a role in anterior scapula development (Kuijper et al., 2005), and *Pax1* is needed for acromion formation (Grüneberg, 1950; Timmons et al., 1994). None of these are known atRA target genes, although Pellegrini and colleagues (2001) have suggested that *Emx2* expression could be indirectly affected by atRA via the induction of *Hoxc6*. Expression of *Sox9* is essential for initiating chondrocyte condensation and for chondroblast differentiation, and it regulates the expression of *Col2a1* that is expressed in cells committed to enter chondrogenesis. Vitamin A is implicated as a player in the process of chondrocyte differentiation (Weston et al., 2003), and atRA has been shown to regulate *Sox9* expression in primary cultures of isolated mouse rib primary cartilage (Sekiya et al., 2001) and limb mesenchyme (Weston et al., 2002). Thus, VAD could affect formation of the scapula and the acromion process by altering chondrocyte condensation and/or differentiation. The first vestige of the acromion, as detected by the expression of *Col2a1* mRNA, is found at E11.5 in the mouse (Timmons et al., 1994) or approximately E13–13.5 in rat. Therefore, the time when VAD is induced in rat fetuses overlaps the time when the acromion would be forming. The defects in the pectoral and pelvic regions in late VAD rat fetuses are unique, as they are not observed in either the early VAD rat model or in other genetic models that disrupt RAR signaling (Table 5). The novel effects on skeletal development observed in the late VAD fetuses further support the idea that this model provides the most stringent negative effect on vitamin A signaling when compared to the genetic models studied to date.

In summary, we have developed a new model that can be used to study the effects of embryonic vitamin A deficiency in the rat after E10.5 of development. The fetal vitamin A deficiency syndrome produced in this model is of similar severity across affected fetuses, and many defects are completely penetrant. Using this approach, we have assigned new functions for vitamin A in the developing skeleton in relation to the timing of deficiency, and we have revealed unique defects that can be attributed to late VAD. The nutritional model described herein enables deficiency to be induced at a defined developmental time, and can be used to study the role of vitamin A in the detailed development of organ systems in the future.

Acknowledgments

We thank Dr. Y. Lee from the Department of Anatomy, R. Sullivan from the RARC for useful discussions on heart/aortic arch development, J. Ahrens in our group for generating the *Wnt3a* riboprobe, L. Vanderploeg from the Biochemistry Media lab for the artwork, and W. Nehls and his staff in the Dept. of Biochemistry animal care unit for their support. This work was funded in part by the U.S. Department of Agriculture HATCH grant (CSREES-WISO4768).

Appendix A. Supplementary data

Supplementary data associated with this article can be found, in the online version, at doi:10.1016/j.ydbio.2007.10.018.

References

Arens, J.F., van Dorp, D.A., 1946a. Activity of 'vitamin A-acid' in the rat. Nature 158, 622–623.

Arens, J.F., van Dorp, D.A., 1946b. Synthesis of some compounds possessing vitamin A activity. Nature 157, 190–191.

Barrow, J.R., Capecchi, M.R., 1996. Targeted disruption of the *Hoxb-2* locus in mice interferes with expression of *Hoxb-1* and *Hoxb-4*. Development 122, 3817–3828.

Chambers, D., Wilson, L., Maden, M., Lumsden, A., 2007. RALDH-independent generation of retinoic acid during vertebrate embryogenesis by CYP1B1. Development 134, 1369–1383.

Chen, J.M., 1952. Studies on the morphogenesis of the mouse sternum: I. Normal embryonic development. J. Anat. 86, 373–386.

Clagett-Dame, M., DeLuca, H.F., 2002. The role of vitamin A in mammalian reproduction and embryonic development. Annu. Rev. Nutr. 22, 347–381.

Condie, B.G., Capecchi, M.R., 1994. Mice with targeted disruptions in the paralogous genes *hoxa-3* and *hoxd-3* reveal synergistic interactions. Nature 370, 304–307.

Dolle, P., Ruberte, E., Leroy, P., Morriss-Kay, G., Chambon, P., 1990. Retinoic acid receptors and cellular retinoid binding proteins: I. A systematic study of their differential pattern of transcription during mouse organogenesis. Development 110, 1133–1151.

Duester, G., Mic, F.A., Molotkov, A., 2003. Cytosolic retinoid dehydrogenases govern ubiquitous metabolism of retinol to retinaldehyde followed by tissue-specific metabolism to retinoic acid. Chem.-Biol. Interact. 143–144, 201–210.

Dupe, V., Matt, N., Garnier, J.M., Chambon, P., Mark, M., Ghyselinck, N.B., 2003. A newborn lethal defect due to inactivation of retinaldehyde dehydrogenase type 3 is prevented by maternal retinoic acid treatment. Proc. Natl. Acad. Sci. U. S. A. 100, 14036–14041.

Eckey, M., Moehren, U., Baniahmad, A., 2003. Gene silencing by the thyroid hormone receptor. Mol. Cell. Endocrinol. 213, 13–22.

Evans, H.M., 1928. The effects of inadequate vitamin A on the sexual physiology of the female. J. Biol. Chem. 77, 651–654.

Fan, X., Molotkov, A., Manabe, S., Donmoyer, C.M., Deltour, L., Foglio, M.H., Cuenca, A.E., Blaner, W.S., Lipton, S.A., Duester, G., 2003. Targeted disruption of Aldh1a1 (Raldh1) provides evidence for a complex mechanism of retinoic acid synthesis in the developing retina. Mol. Cell. Biol. 23, 4637–4648.

Grondona, J.M., Kastner, P., Gansmuller, A., Decimo, D., Chambon, P., Mark, M., 1996. Retinal dysplasia and degeneration in RARbeta2/RARgamma2 compound mutant mice. Development 122, 2173–2188.

Grüneberg, H., 1950. Genetical studies on the skeleton of the mouse: II. Undulated and its "modifiers". J. Genet. 50, 142–173.

Ikeya, M., Takada, S., 2001. Wnt-3a is required for somite specification along the anteroposterior axis of the mouse embryo and for regulation of cdx-1 expression. Mech. Dev. 103, 27–33.

Jackson, B., Kinsey, V., 1946. The relation between maternal vitamin A intake, blood level, and ocular abnormalities in the offspring of the rat. Am. J. Ophthalmol. 29, 1234–1242.

Kaiser, M.E., Merrill, R.A., Stein, A.C., Breburda, E., Clagett-Dame, M., 2003. Vitamin A deficiency in the late gastrula stage rat embryo results in a one to two vertebral anteriorization that extends throughout the axial skeleton. Dev. Biol. 257, 14–29.

Kaufman, M.H., 1992. The Atlas of Mouse Development. Academic Press, London.

Kuijper, S., Beverdam, A., Kroon, C., Brouwer, A., Candille, S., Barsh, G., Meijlink, F., 2005. Genetics of shoulder girdle formation: roles of *Tbx15* and *aristaless*-like genes. Development 132, 1601–1610.

Lohnes, D., Kastner, P., Dierich, A., Mark, M., LeMeur, M., Chambon, P., 1993. Function of retinoic acid receptor gamma in the mouse. Cell 73, 643–658.

Lohnes, D., Mark, M., Mendelsohn, C., Dolle, P., Dierich, A., Gorry, P., Gansmuller, A., Chambon, P., 1994. Function of the retinoic acid receptors (RARs) during development (I). Craniofacial and skeletal abnormalities in RAR double mutants. Development 120, 2723–2748.

Lufkin, T., Mark, M., Hart, C.P., Dolle, P., LeMeur, M., Chambon, P., 1992. Homeotic transformation of the occipital bones of the skull by ectopic expression of a homeobox gene. Nature 359, 835–841.

Maeda, Y., Dave, V., Whitsett, J.A., 2007. Transcriptional control of lung morphogenesis. Physiol. Rev. 87, 219–244.

Manley, N.R., Capecchi, M.R., 1997. *Hox* group 3 paralogous genes act synergistically in the formation of somatic and neural crest-derived structures. Dev. Biol. 192, 274–288.

Mark, M., Lufkin, T., Vonesch, J.L., Ruberte, E., Olivo, J.C., Dolle, P., Gorry, P., Lumsden, A., Chambon, P., 1993. Two rhombomeres are altered in *Hoxa-1* mutant mice. Development 119, 319–338.

Mark, M., Ghyselinck, N.B., Chambon, P., 2006. Function of retinoid nuclear receptors: lessons from genetic and pharmacological dissections of the retinoic acid signaling pathway during mouse embryogenesis. Annu. Rev. Pharmacol. Toxicol. 46, 451–480.

Matt, N., Dupe, V., Garnier, J.M., Dennefeld, C., Chambon, P., Mark, M., Ghyselinck, N.B., 2005. Retinoic acid-dependent eye morphogenesis is orchestrated by neural crest cells. Development 132, 4789–4800.

McCaffery, P., Drager, U.C., 2000. Regulation of retinoic acid signaling in the embryonic nervous system: a master differentiation factor. Cytokine Growth Factor Rev. 11, 233–249.

Mendelsohn, C., Lohnes, D., Decimo, D., Lufkin, T., LeMeur, M., Chambon, P., Mark, M., 1994. Function of the retinoic acid receptors (RARs) during development (II). Multiple abnormalities at various stages of organogenesis in RAR double mutants. Development 120, 2749–2771.

Moise, A.R., Noy, N., Palczewski, K., Blaner, W.S., 2007. Delivery of retinoid-based therapies to target tissues. Biochemistry 46, 4449–4458.

Molotkov, A., Molotkova, N., Duester, G., 2006. Retinoic acid guides eye morphogenetic movements via paracrine signaling but is unnecessary for retinal dorsoventral patterning. Development 133, 1901–1910.

Niederreither, K., McCaffery, P., Drager, U.C., Chambon, P., Dolle, P., 1997. Restricted expression and retinoic acid-induced downregulation of the retinaldehyde dehydrogenase type 2 (RALDH-2) gene during mouse development. Mech. Dev. 62, 67–78.

Pellegrini, M., Pantano, S., Fumi, M.P., Lucchini, F., Forabosco, A., 2001. Agenesis of the scapula in *Emx2* homozygous mutants. Dev. Biol. 232, 149–156.

Qu, S., Tucker, S.C., Zhao, Q., deCrombrugghe, B., Wisdom, R., 1999. Physical and genetic interactions between *Alx4* and *Cart1*. Development 126, 359–369.

Quadro, L., Hamberger, L., Gottesman, M.E., Wang, F., Colantuoni, V., Blaner, W.S., Mendelsohn, C.L., 2005. Pathways of vitamin A delivery to the embryo: insights from a new tunable model of embryonic vitamin A deficiency. Endocrinology 146, 4479–4490.

Ramírez-Solis, R., Zheng, H., Whiting, J., Krumlauf, R., Bradley, A., 1993. *Hoxb-4* (*Hox-2.6*) mutant mice show homeotic transformation of a cervical vertebra and defects in the closure of the sternal rudiments. Cell 73, 279–294.

Roberts, A.B., DeLuca, H.F., 1967. Pathways of retinol and retinoic acid metabolism in the rat. Biochem. J. 102, 600–605.

Roelen, B.A., de Graaff, W., Forlani, S., Deschamps, J., 2002. *Hox* cluster polarity in early transcriptional availability: a high order regulatory level of clustered *Hox* genes in the mouse. Mech. Dev. 119, 81–90.

Rossant, J., Zirngibl, R., Cado, D., Shago, M., Giguere, V., 1991. Expression of a retinoic acid response element-hsplacZ transgene defines specific domains of transcriptional activity during mouse embryogenesis. Genes Dev. 5, 1333–1344.

Ruberte, E., Dolle, P., Krust, A., Zelent, A., Morriss-Kay, G., Chambon, P., 1990. Specific spatial and temporal distribution of retinoic acid receptor gamma transcripts during mouse embryogenesis. Development 108, 213–322.

Ruberte, E., Dolle, P., Chambon, P., Morriss-Kay, G., 1991. Retinoic acid receptors and cellular retinoid binding proteins: II. Their differential pattern of transcription during early morphogenesis in mouse embryos. Development 111, 45–60.

Sekiya, I., Koopman, P., Tsuji, K., Mertin, S., Harley, V., Yamada, Y., Shinomiya, K., Niguji, A., Noda, M., 2001. Transcriptional suppression of Sox9 expression in chondrocytes by retinoic acid. J. Cell. Biochem. 81, 71–78.

Thompson, J.N., Howell, J.M., Pitt, G.A., 1964. Vitamin A and reproduction in rats. Proc. R. Soc. London, Ser. B Biol. Sci. Biol. Sci. 159, 510–535.

Timmons, P.M., Wallin, J., Rigby, P.W., Balling, R., 1994. Expression and function of Pax 1 during development of the pectoral girdle. Development 120, 2773–2785.

Ulven, S.M., Gundersen, T.E., Weedon, M.S., Landaas, V.O., Sakhi, A.K., Fromm, S.H., Geronimo, B.A., Moskaug, J.O., Blomhoff, R., 2000. Identification of endogenous retinoids, enzymes, binding proteins, and receptors during early postimplantation development in mouse: important role of retinal dehydrogenase type 2 in synthesis of all-*trans*-retinoic acid. Dev. Biol. 220, 379–391.

Wang, Z., Dolle, P., Cardoso, W.V., Niederreither, K., 2006. Retinoic acid regulates morphogenesis and patterning of posterior foregut derivatives. Dev. Biol. 297, 433–445.

Warkany, J., Roth, C.B., 1948. Congenital malformations induced in rats by maternal vitamin A deficiency: II. Effect of varying the preparatory diet upon the yield of abnormal young. J. Nutr. 35, 1–11.

Warkany, J., Schraffenberger, E., 1944. Congenital malformations of the eyes induced in rats by maternal vitamin A deficiency. Proc. Soc. Exp. Biol. Med. 57, 49–52.

Warkany, J., Schraffenberger, E., 1946. Congenital malformations induced in rats by maternal vitamin A deficiency: I. Defects of the eye. Arch. Ophthalmol. 35, 150–169.

Warkany, J., Roth, C.B., Wilson, J.G., 1948. Multiple congenital malformations: a consideration of etiologic factors. Pediatrics 1, 462–471.

Weston, A.D., Chandraratna, R.A., Torchia, J., Underhill, T.M., 2002. Requirement for RAR-mediated gene repression in skeletal progenitor differentiation. J. Cell Biol. 158, 39–51.

Weston, A.D., Hoffman, L.M., Underhill, T.M., 2003. Revisiting the role of retinoid signaling in skeletal development. Birth Defects Res. C Embryo Today 69, 156–173.

White, J.C., Shankar, V.N., Highland, M., Epstein, M.L., DeLuca, H.F., Clagett-Dame, M., 1998. Defects in embryonic hindbrain development and fetal resorption resulting from vitamin A deficiency in the rat are prevented by feeding pharmacological levels of all-*trans*-retinoic acid. Proc. Natl. Acad. Sci. U. S. A. 95, 13459–13464.

White, J.C., Highland, M., Clagett-Dame, M., 2000. Abnormal development of the sinuatrial venous valve and posterior hindbrain may contribute to late fetal resorption of vitamin A-deficient rat embryos. Teratology 62, 374–384.

Wilson, J.G., Warkany, J., 1948. Malformations in the genito-urinary tract induced by maternal vitamin A deficiency in the rat. Am. J. Anat. 83, 357–407.
Wilson, J.G., Warkany, J., 1949. Aortic-arch and cardiac anomalies in the offspring of vitamin A deficient rats. Am. J. Anat. 85, 113–155.
Wilson, J.G., Roth, C.B., Warkany, J., 1953. An analysis of the syndrome of malformations induced by maternal vitamin A deficiency. Effects of restoration of vitamin A at various times during gestation. Am. J. Anat. 92, 189–217.
Zile, M.H., 2001. Function of vitamin A in vertebrate embryonic development. J. Nutr. 131, 705–708.